DESIGN AND DEVELOPMENT OF HEAT EXCHANGER BASED ON OPEN CELL METAL FOAM

ANANTHASAYANAM SUBRAMANI SHARATH

FACULTY OF ENGINEERING
UNIVERSITY OF MALAYA
KUALA LUMPUR

2019

DESIGN AND DEVELOPMENT OF HEAT EXCHANGER BASED ON OPEN CELL METAL FOAM

ANANTHASAYANAM SUBRAMANI SHARATH

THESIS SUBMITTED IN FULFILMENT OF THE REQUIREMENTS FOR THE DEGREE OF MASTERS OF MECHANICAL ENGINEERING

FACULTY OF ENGINEERING
UNIVERSITY OF MALAYA
KUALA LUMPUR

2019

UNIVERSITY OF MALAYA

ORIGINAL LITERARY WORK DECLARATION

Name of Candidate: Ananthasayanam subramani sharath

Matric No: KQK170015

Name of Degree: Masters of Mechanical Engineering

Title of Research Report : Design and Development of heat exchanger based on open cell metal foam

Field of Study: Heat transfer and Thermo fluids

I do solemnly and sincerely declare that:

(1) I am the sole author/writer of this Work;
(2) This Work is original;
(3) Any use of any work in which copyright exists was done by way of fair dealing and for permitted purposes and any excerpt or extract from, or reference to or reproduction of any copyright work has been disclosed expressly and sufficiently and the title of the Work and its authorship have been acknowledged in this Work;
(4) I do not have any actual knowledge nor do I ought reasonably to know that the making of this work constitutes an infringement of any copyright work;
(5) I hereby assign all and every rights in the copyright to this Work to the University of Malaya ("UM"), who henceforth shall be owner of the copyright in this Work and that any reproduction or use in any form or by any means whatsoever is prohibited without the written consent of UM having been first had and obtained;
(6) I am fully aware that if in the course of making this Work I have infringed any copyright whether intentionally or otherwise, I may be subject to legal action or any other action as may be determined by UM.

Candidate's Signature Date:

Subscribed and solemnly declared before,

Witness's Signature Date:

Name:

Designation:

DESIGN AND DEVELOPMENT OF HEAT EXCHANGER BASED ON OPEN CELL METAL FOAM

ABSTRACT

The fluid flowing through pipes or ducts is commonly used in heating and were the liquids or the gas. The fluid in this type of flow is usually forced by a blower to bring about the preferred heat transfer. The equipment's that ease this process are the Heat Exchangers. The Copper metal foams with 60 PPI (Pores Per Inch) was chosen to develop the Heat Exchanger. The primary objective of the research in developing a compact metal foam heat exchanger in different configuration was achieved. Firstly, the Design 1 was a type of Heat Exchanger that the copper metal foams and the aluminum fins are arranged consecutively and closely packed. Secondly, the Design 2 was a type of Heat Exchanger that the pair of aluminum fins and foams were arranged with air gap of 5mm in between. The Novelty of this research lies with the Different design and the configuration of the metal foam arranged in the housing with the maximum pore density of 60 PPI. The Experimental Investigation of both the designs were studied separately based on the Velocity Profile, Pressure Drop, Heat transfer coefficient and the Temperature Difference. The effects of each mentioned above were studied and analyzed by varying velocity from 0.8m/s to 2.3m/s. The experiments were conducted under steady state conditions of maintaining the constant room temperature and the constant heat flux of 50˚C. The Heat transfer characteristics of each localized points from $\mathbf{H_{11}}$ to $\mathbf{H_{51}}$ and $\mathbf{H_{12}}$ to $\mathbf{H_{52}}$ in the heat exchanger for both the design1 and 2 were studied thoroughly. The average Nusselt number for both designs was evaluated based on the average heat transfer coefficient and has been compared with the analytical equation and the previous study.

Keywords : Heat Exchangers, Heat transfer coefficient, Velocity Profile, Pressure Drop, Temperature Difference

REKA BENTUK DAN PENGHASILAN HEAT EXCHANGER BERDASARKAN OPEN CELL METAL FOAM

ABSTRAK

Dalam proses pemanasan, bendalir seperti cecair atau gas yang mengalir melalui paip atau saluran biasa digunakan. Pemindaahan haba oleh bendalir selalunya dihasilkan oleh blower. Proses ini dapat dimudahkan dengan heat exchanger. Heat exchanger yang telah dipilih untuk kajian ini adalah logam kuprum (60 PPI). Objektif utama dalam penyelidikan ini adalah untuk menyediakan metal foam yang berbeza konfigurasi untuk heat exchanger. Terdapat dua reka bentuk konfigurasi yang dihasilkan iaitu yang pertama metal foam disusun dengan rapat secara berselang seli dengan aluminum fins. Manakala yang kedua, metal foam dan aluminum fins disusun berselang seli dangan jarak 5mm. Ketulinan kajina ini dapat dilihat melalui reka bentuk konfigurasi metal foam yang berbeza menggunakan pori metal foam dengan bacaan maksimum 60 PPI. Kajian ini dianalis berdasarkan empat factor iaitu Velocity Profile, Pressure Drop, Heat transfer coefficient dan Temperature Difference. Faktor-faktor tersebut dikaji dan dianalisi mengikut kelajuan yang berbeza-beza dari 0.8m/s hingga 2.3m/s. Kajian ini dijalankan dalam keadaan stabil dengan mngekalkan suhu ruang yang sama dan heat flux tetap 50˚C. Ciri-ciri pemindahan haba dari titik $\mathbf{H_{11}}$ ke $\mathbf{H_{51}}$ dan $\mathbf{H_{12}}$ hingga $\mathbf{H_{52}}$ untuk kedua-dua reka bentuk konfigurasi heat exchanger dikaji sepenuhnya. Purata bilangan Nusselt untuk kedua-dua reka bentuk dinilai berdasarkan purata heat transfer coefficient dan dibandingkan dengan analytical equation dan kajian terdahulu.

Kata kunci: Heat Exchangers, Heat transfer coefficient, Velocity Profile, Pressure Drop, Temperature Difference

ACKNOWLEDGEMENTS

God has a reason for allowing things to happen. God is great. I would like to express my deepest appreciation to all and sundry who postulated to complete this study. A special gratitude to my supervisor Dr. Poo Balan Ganesan, who have helped me to coordinate by giving stimulating encouragement by monitoring continuously. Furthermore, I would like to acknowledge my team members Fathiah Zaib, PhD student and Deanish Ramaya, undergraduate student who have helped to complete this study. A special thanks to my father, mother and my sister who have supported me from the beginning to complete this course. A specific mention about my friend Ramesh Nayaka, PhD scholar who had taught me about basics of research. I would like to extend my thanks to all the master classmates Rakesh, Chandra, Gaston for their verbal support all the time.

TABLE OF CONTENTS

LIST OF FIGURES

LIST OF TABLES

LIST OF SYMBOLS AND ABBREVIATIONS

Δp	:	Pressure drop of the specimen
h_o	:	Heat transfer coefficient at the outer diameter
h_i	:	Heat transfer coefficient at the inner diameter
Re	:	Reynolds number
Pr	:	Prandtl number
Nu	:	Nusselt number
m	:	Mass flow rate of the fluid
v	:	Average Inlet Velocity of the fluid
C_p	:	Specific heat capacity of the fluid
ϵ	:	Enhancement Efficiency
q	:	Heat flux of the cartridge heater
T_{in}	:	Temperature of the Inlet fluid in the test section
T_{out}	:	Temperature of the Outlet fluid in the test section
T_{amb}	:	Ambient temperature of the fluid in the test section
S	:	Total Heat transfer area of the porous media
A_b	:	Area of the base plate
V	:	Voltage supply to the heater
I	:	Current supply to the heater
d_p	:	Average pore diameter of the metal foam
d_h	:	Spherical diameter of the pore
V	:	Volume of the metal foam used
Q_{loss}	:	Heat lost to the fluid from the heater
Q_{air}	:	Heat transferred to the working fluid
A	:	Heat transfer area

A_1	:	Heat transfer area of Design 1
A_2	:	Heat transfer area of Design 2
hn_1	:	Heat transfer coefficient at the localized point 1 in Design 1
hn_2	:	Heat transfer coefficient at the localized point 1 in Design 2
H_{n1}	:	Average heat transfer coefficient of the Design 1
H_{n2}	:	Average heat transfer coefficient of the Design 2
H_1	:	Overall heat transfer coefficient of Design 1
H_2	:	Overall heat transfer coefficient of Design 2
ε	:	Porosity of the Metal foam used
K_c	:	Thermal conductivity of copper
K_f	:	Thermal conductivity of the fluid
K_{Al}	:	Thermal conductivity of aluminum
v_1	:	Velocity Profile of the Design 1
v_2	:	Velocity Profile of the Design 2
P_1	:	Pressure Drop of Design 1
P_2	:	Pressure Drop of Design 2
D_h	:	Hydraulic Diameter of the test section
Q_{in}	:	Input power given to the heater
T_w	:	Surface temperature of the wall
T_b	:	Bulk fluid temperature
ΔT	:	Temperature Difference of the Outlet and inlet fluid
HE	:	Heat Exchanger
PCM	:	Phase Change Material
PPI	:	Pores Per Inch
TIM	:	Temperature Interface Material
PMMA	:	Polymethyl Methacrylate

WEDM	:	Wire Electric Discharge Machining
IC	:	Internal Combustion
CFD	:	Computational Fluid Dynamics
ABS	:	Acrylonitrile Butadiene Styrene
EPR	:	Energy Performance Ratio
AR	:	Aspect Ratio
CAD	:	Computer Aided Design
W-EDM	:	Wire Electric Discharge Machining
TIM	:	Temperature Interface Material
TIG	:	Tungsten Inert Gas
RTD	:	Resistance Temperature Detector

LIST OF APPENDICES

CHAPTER 1: INTRODUCTION

1.1 Project Background

The purest sense has been around since man started cooking in pots and ovens are Heat Exchangers (HE). Fundamentally, the three ways that the heat is transferred to other medium are convection, conduction and radiation. The early heat exchangers were simply rocks placed in fire which was moved inside a small room to stabilize the interior without causing fire. The heat transfer area absorbs the heat from the fire which in turn heats the interior of the residence. The same principle was used in the development of hot water bottle. From then on slowly the heat exchangers started to evolve. The initial invention from the romans was central heating. The similar technology was also used by Koreans which was called as Ondol heating. It is believed that over the next five decades hot water and the steam heat exchangers will revolutionize the world. The modern heat exchangers are designed in such a way that it can fit into palm of your hand. Heat exchangers are now a days used in all industries like air conditioning and refrigeration, petrochemical industries, food and drink and even in pharmaceutical manufacturing. Heat exchangers now arrived the market in different varieties each of them to serve different purpose. There are different types of HE which have converted like shell and tube to plate and shell. Similarly, the adiabatic wheel and the pillow plate have been developed to regenerative models. Additionally, each heat exchanger can be classified based on the fluid pass through it. The type of materials generally used are gas to liquid / liquid or solid to phase change. However, from the beginning of boiling pot and brick oven the heat exchangers have come long way. The renewable power will be easily accessible to all the places around the world. The energy from sun and the other from earth (geothermal) energy plays a considerable role. The classic example for heat exchanger which most of all would have known is coolant where it is the circulating fluid flowing through the radiator in an Internal combustion (IC) engine. The cold fuel in engine's oil system is

heated from the transferred heat in the commercial aircraft heat exchanger. This is done to improvise the efficiency which reduces the possibility of water deceived in the fuel.

Heat exchangers are designed in such a way that resistance for the fluid flow is minimized by maximizing between two fluids in the wall surface area. The HE performance can also be affected by addition of fins or the corrugations either in one or both directions which increases the surface area and the channel fluid flow or induce turbulence. The Figure1.1 shown below is the aluminum metal foam heat exchanger with the fins in between. The metal foams have better permeability and high heat transfer than the flat surface metal or any other type.

Figure 1.1: Metal foam Heat exchanger

1.2 Problem Statement

After the invention of the Heat Exchanger (HE) took place from there had been facing many problems by the engineers. The common problems faced by engineers in HE was vibration in the heat transfer area, exchanger leakage and fouling etc. These problems are the signs of a poor performance of a heat exchanger. Considering the invention of open cell metal foam heat exchangers had comparatively shown improvements than the tube bundle type.

Past research has been done in metal foam by analyzing the structures, density of the foam in terms of Pores Per Inch (PPI) by varying it. The investigation of the influence of fluid characteristics, flow arrangement, material selection and extending the heat transfer area. There are only two papers published on wet air metal foams which mainly focusses on the heat transfer coefficient and pressure drop. The results show that the heat transfer increase with increasing the PPI. It has more significant effect on rate of heat transfer than the porosity. The previous study in most forced convection applications carried improvements by maximizing the heat transfer coefficient while minimizing the pressure drop and the temperature difference.

1.3 Project Objectives

The project objectives that were identified based on the background study and the present-day problems in the Heat exchangers.

i. To develop the two different configuration type of heat exchanger based on open cell metal foam.
ii. To conduct the experimental investigation and determine the characteristics of pressure drop and heat transfer coefficient of the developed heat exchanger.

1.4 Project Scope

The gas filled pores comprising of large portion of the volume like cellular structure are called metal foams. The ultralight metal capability is because of the 5-25% high porosity from the base metal. These metal foams retain some of the physical properties typically from the base metal. The heat exchangers are used to transfer or exchange heat from one to another which basically works on the principle of conduction and convection. The scope of the research work is to develop a forced convection wind tunnel with open cell metal foam heat exchanger. The metal foam HE is designed and fabricated in different configuration to study and analyze the experimental investigation. The two factors which

define the efficiency of HE is heat transfer coefficient and the pressure drop where in the later stages will be verified to calculate the efficiency of the HE. The research is carried out in the copper metal foam for the different configurations. The metal foams with different PPI will be used to compare for the better efficiency. The heat transfer coefficient **(h)** and the pressure drop **(Δp)** changes inside the test rig will analyzed by varying the velocity for different PPI of the metal foam. The Figure1.2 shows the copper metal foam and the pores are densely formed. The figure is captured image of a portion of the metal foam structure that can be in any form like block or circular structure.

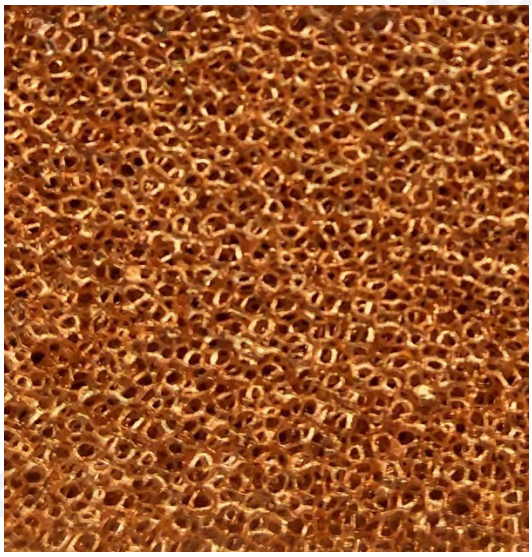

Figure 1.2: Metal foam with 60 PPI

CHAPTER 2: LITERATURE REVIEW

2.1 Compact Metal Foam Heat Exchangers

In recent times various configurations particularly, the single U – tube ground heat exchangers was analyzed on the improvement of the performance of the ground heat exchangers. The novelty of this paper was comparison between single U tube and helical heat exchangers that are in eight types. The numerical simulations were performed by CFD (Computational Fluid Dynamics). This study has done nine different types of configuration in terms of heat exchange rate, effectiveness, pressure drop and thermal resistance. The results show that the outlet water temperature in helix tube, double helix tube and triple helix are less considerably less than the other types. The temperature difference of triple helix exchanger is almost two times higher than helix U- tube. The best thermal performance with other ground heat exchangers was the triple helix heat exchangers. It was concluded that the Single U-tube heat exchanger has the poor thermal performance when compared to other types. (Javadi, Mousavi Ajarostaghi, Pourfallah, & Zaboli, 2019)

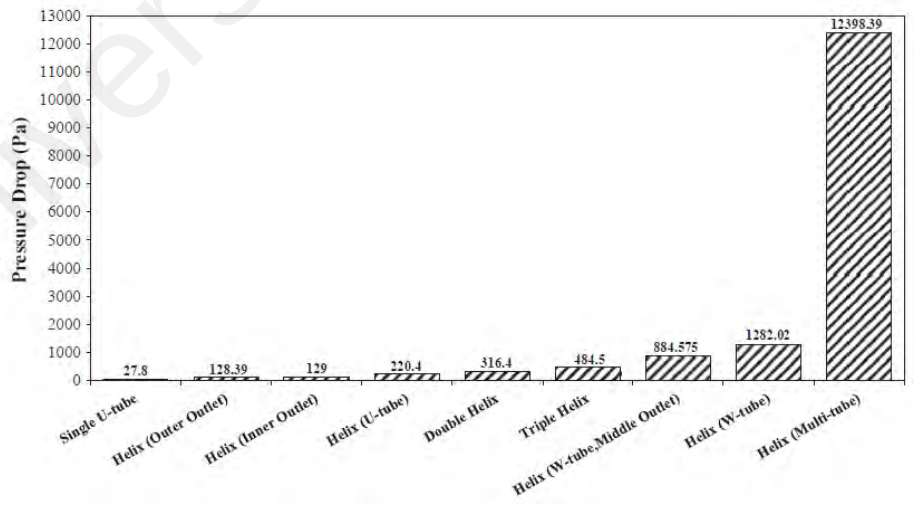

Figure 2.1: Thermal performance of different Heat Exchangers

The Figure 2.1 in **(Javadi et al., 2019)** shows the thermal performance of the different heat exchangers.

The study explains about the design and performance of a compact tubular manifold microchannel heat exchanger which was not in the types of the HE that the research carry out.(Javadi et al., 2019). The point of this investigation was to encounter the job of progressively exact stream dissemination utilizing an additively made complex for single stage stream under low to direct warmth motion conditions. The working liquid was water and 3D printed complex which was made of ABS (Acrylonitrile Butadiene Styrene) plastic was utilized to appropriately circulate the stream. The Reynolds number was fluctuated somewhere in the range of 250 and 630. The weight drop inside the test area was shifted from 0.1 bar to 0.7 bar for the test conditions. The weight drop in the test segment increments as the mass stream rate increments. The shell side warmth exchange coefficient was found between 28000 – 45000 W/m2K with water as the working liquid.The overall heat transfer coefficient for the heat exchanger was nearly 25000 W/m^2K.(Tiwari, Andhare, Shooshtari, & Ohadi, 2019)

2.2 Open cell metal foam

The numerical examination depends on the assessment of warm and liquid dynamic of a minimized heat exchanger in aluminum froth. The point of the examination was to discover the element of the heat exchanger measurements for the assessment of heat exchange and to expand the weight drop. The aftereffects of the investigation demonstrate that the ideal froth thickness of the cylinder measurement was equivalent to 5. The Energy Performance Ratio (EPR) was additionally assessed. The outcomes demonstrate the warmth exchange control increments with the expansion in Reynolds number. For the lower Reynolds number, the estimation of higher warmth exchange is accomplished. The foam has been modelled assuming the local thermal non equilibrium model.(Buonomo, Pasqua, Ercole, & Manca, 2018)

Direct numerical recreation of transport in froth materials can profit by practical portrayals of the permeable medium geometry created by utilizing non-dangerous 3D imaging procedures. X-beam microtomography utilizes PC handled X-beams to create tomographic pictures or cuts of explicit districts of the item under scrutiny, and is in a perfect world appropriate for imaging murky and complex permeable media. In this work, we utilize miniaturized scale CT for numerical investigation of wind stream and convection through four diverse high-porosity copper froths. Every one of the four froth tests display roughly a similar relative thickness (6.4– 6.6% strong volume portion), yet have distinctive pore densities (5, 10, 20, and 40 pores for every inch, PPI). A business smaller scale figured tomography scanner is utilized for examining the 3D microstructure of the froths at a goals of 20 lm, yielding heaps of two-dimensional pictures. These pictures are prepared so as to reproduce and work the genuine, arbitrary structure of the froths, whereupon recreations are led of constrained convection through the pore spaces of the metal tests.(Diani, Bodla, Rossetto, & Garimella, 2015)

The study is involved with the metal foams that are filled inside the tube has the greater effect on heat transfer. These tubes filled with the metal foams promote high heat transfer by providing a high surface area. The working fluid used here was the R245fa refrigerant with the mass flux ranging from 200 to 10000 Kg/m^2s. The foam filled tube was investigated for the heat transfer rate and the pressure drop. The Heat loss from the tube was measured by

$$\mathbf{Qloss = v \times I - \dot{m}\,(ho - hi)} \qquad \textbf{Equation 1}$$

Where Q_{loss} is the heat lost from the tube, v is the Voltage supply, I is the current supply, h_o and h_i are the enthalpy at outlet and inlet respectively. The results show that the decreasing the microchannels cross sectional area causes most of the predictive

methods to fail that was explained by imperfections of the of the pore.(Bamorovat Abadi & Kim, 2017)

The preference of metal foam is also high towards the aluminum foam and this study is the experimental investigation of the convective heat transfer in open cell foams. The aluminum foam samples of 40 PPI with porosity 93% was used to determine the intrinsic properties of this foam with air velocity being varied from 1 to 5 m/s for two height of porous block 16mm and 20mm respectively. The experiments were investigated with the calculation of the heat transfer and the pressure drop in the direction of flow. The enhancement efficiency of each block were also calculated and investigated and the results show that sample grades of foam 40 PPI and height 20mm create less pressure drop than solid blocks of height 16mm. The results reveals that increasing the size of the metallic foams blocks can boost the turbulent kinetic energy levels. When compared to solid baffles the metal foams creates less pressure losses because of the permeability.

$$\epsilon = \frac{\dot{m}\, cp\, (To - Tin)}{u\, A\, \Delta P} \qquad \textbf{Equation 2}$$

Where ϵ is the enhancement efficiency, $\dot{m}$ is the mass flow rate of the air, T_o is the outlet temperature, T_{in} is the inlet temperature, u is the inlet velocity, A is the surface area of the foam, and ΔP is the pressure drop across the blocks. The effect of inserting the metal foams in turbulent air improves the heat transfer by 300% compared with the empty channel which reduces the power supplied.(Hamadouche, Nebbali, Benahmed, Kouidri, & Bousri, 2016)

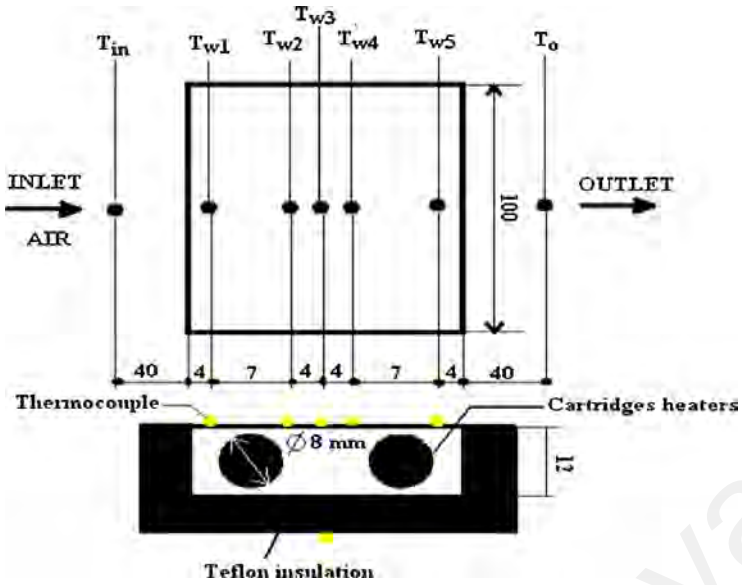

Figure 2.2: Thermocouples placed along the wall towards the flow direction

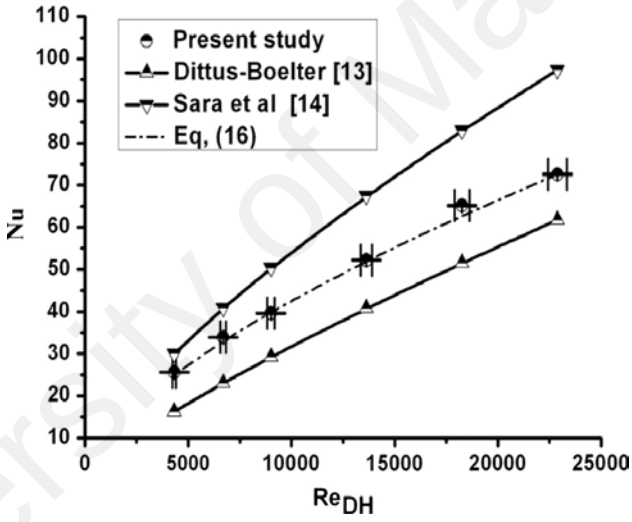

Figure 2.3: Comparison of Nu between Present and Previous study

The Figure 2.2 and Figure 2.3 in **(Hamadouche et al., 2016)** shows the comparison of present and the previous work comparison.

The accompanying examination is a correlation between the metal froth heat exchanger with and without balances. Open cell metal froth is favored the most due to its porosity and high warmth exchange applications. The perceptible model comprising of Darcy – Forchimer brinkman stream model and warm non - balance vitality model is utilized to perform to dimensional reproductions on the metal froth. The warm structure

of the warmth exchangers is dependably a tradeoff between warmth exchange and weight drop. The tests were done between exposed cylinder group and a finned warmth exchanger as far as weight drop and warmth exchange coefficient. Each froth differing from 10 PPI until 45PPI were utilized to play out the correlation. It was recently tried in a breeze burrow fluctuating with various speeds from 1.2m/s to 3.2m/s. The blade pitch of every wa 1.4mm with a thickness of 0.115mm. For a similar mass stream rate metal froth with a high pore thickness is exchanging more warmth than the blades. The frothed warmth exchangers appear at multiple times higher warmth exchange than the uncovered cylinder and the group at a similar fan control. In any case, a metal froth heat exchanger can beat the finned warmth exchanger if the frontal zone is changed. Thus this study shows the potential of a open cell metal foam for high performance heat exchanger designs.(Huisseune, De Schampheleire, Ameel, & De Paepe, 2015)

It is notable that the assembling procedure of open-cell froths marginally prolongs their swaggers in a single bearing, accordingly making them anisotropic; thus, anisotropy influences froth attributes. Besides, real froths can be described with reference to a Representative Volume Element (RVE), characterized as the cubic sub-volume having indistinguishable qualities from those of the entire froth. A fittingly picked RVE is exceptionally useful to pass reenactment information from a smaller scale to a large scale. The significant pretended by RVE in describing froths execution recommends further research in its assurance, so as to diminish computational power and to permit to apply the volume-averaging strategy to open-cell froths. In this paper, anisotropy and RVE for the powerful warm conductivity of open-cell metal froths are numerically dissected. In the wake of examining with Computed Tomography (CT) and postprocessing four open-cell aluminum froths with various porosities and similar Pores Per Inch (PPI) esteem, their morphologies are researched so as to assess the impacts of porosity on cells anisotropy. Froth cell stretching is measured by an anisotropy proportion. Reproductions

are performed on CT information with a limited component technique to process the viable warm conductivities along three symmetrical headings, and results are contrasted and information distributed in the writing. Another connection between's compelling warm conductivity, porosity and bearing is displayed.(Iasiello, Bianco, Chiu, & Naso, 2019)

2.2.1 Phase change material (PCM)

The utilization of phase change materials for warm vitality stockpiling is known for its low warm conductivity. The copper particles and the copper froth were utilized to improve the warm conductivity of a Microencapsulated stage change material (MicroPCM). The minor impacts of copper pore size and mass part and the Pore per Inch (PPI) on the warm properties were explored. The substance and microstructures of the PCM were portrayed by fourier change infrared spectroscopy and Scanning electron microscopy. The impact of adding the copper particles to the MicroPCM diminished the inactive warmth with the expanded loadings. The molecule size of the MicroPCM was estimated by laser molecule sizer analyzer (BT-9300H, Bettersize). The warm steadiness examination of the MicroPCM. The precisions of the temperature and enthalpy were in the middle of 0.1˚C and 0.1% individually. The effects of adding the copper particles in the copper foams were investigated in this study. Latent heat of the MicroPCM composites decreased with increasing copper particles mass fraction. The Figure 2.4 shows the thermal conductivity of Micro PCM with varied PPI.(Rao, Wen, & Liu, 2018)

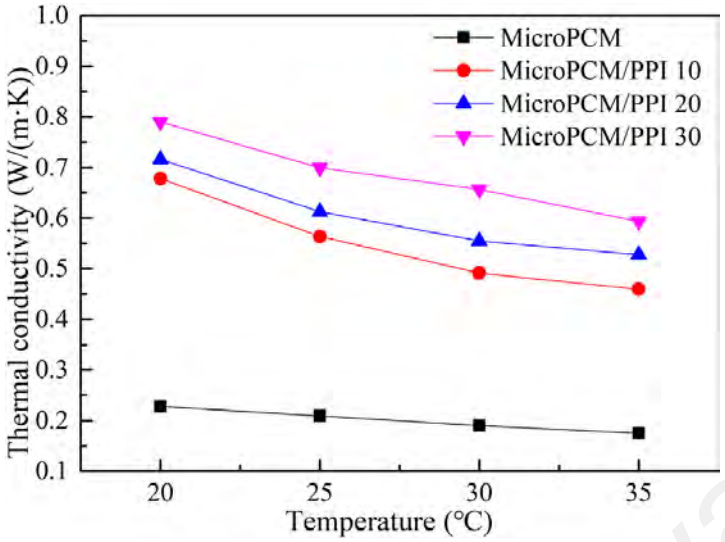

Figure 2.4: Thermal conductivity of MicroPCM with varied PPI

This investigation shows a warmth exchanger model containing PCM material to give a 1KW warming capacity to 2 hours. The warmth exchanger was tried in a shut circle wind burrow which was utilized to consistent speed supply with the temperature changes by which the PCM can be dissolved. The temperature and air speed estimations were recorded for eight distinctive wind stream rate and warming force was evaluated. The auxiliary target of the examination was to give results appropriate approval of the numerical models. The geometry of the model was nitty gritty with the warming force given. The hardening of PCM was troublesome the worldwide conduct of the warmth exchanger was basic. In view of the alterations done the warmth exchange rate expanded in light of the surface region. The wind current for this situation was laminar because of little components of the channels. The results say that a total of 27 Kg of PCM was used for testing which was designed to store enough energy.(Labat, Virgone, David, & Kuznik, 2014)

2.2.2 Effect of adding fins with foams

The balances and metal foam give the more prominent impact of heat exchange which the investigation has been conveyed dependent on that. This examination includes the exploratory examination on the cementing rate of water in metal foams with the balances.

The essential target of the investigation was adding of the fins to the metal foams to see the delayed consequences of the heat exchange. The metal foam tests with various balance interims were taken for the examinations. The procedure of hardening in finned metal foam under base cooling was tentatively completed. The investigation included three unique instances of the foam with various interims and the outcomes demonstrate that the when embeddings of blades existed a surprising distinction. Amid the cementing procedure the interface was level before embeddings the fins and in the wake of embeddings the balances ended up bended. The outcomes demonstrate the impact of embeddings fins into froths obviously affects hardening rate contrasted and unadulterated metal foam condition. Also adding the fin interval by varying in the metal foam does not show any significant effect on the solidification rate when the parameters of pore density and porosity were actually same.(Q. Bai et al., 2018)

Further adding to the point adding fins to the foams this study has been done for the improvement of the fin efficiency of a solid wire fin by oscillating heat pipe. The unit was tried in a breeze burrow by trading the warmth between boiling water streaming inside and the air stream. The bay temperature of sight-seeing was fluctuated somewhere in the range of 40 and 80˚C with the encompassing temperature being steady. The swaying heat pipe balance could advance higher balance effectiveness of the wire on cylinder heat exchanger. The result emerge from the combination of heat transfer from the conduction through the fin body and condensation of fluid inside the capillary tube.(Samana, Kiatsiriroat, & Nuntaphan, 2014)

2.3 Applications of copper metal foams

The preference of using the metal foam has increased because of the applications it provides. This study is the experimentation of the open cell hollow ligament in the metal foams carried at low Reynolds number. Initially the evaluation has been made between

two samples 10 and 20PPI by comparing the Nusselt number at four volumetric rate of heat transfer. The heat flux supplied is varied between 200 to 575 W. The target of the investigation was to evaluate the warmth trade procedure of empty tendons metal froth. After the analyses been completed in the protected shut circle burrow the outcomes demonstrate that multiple times increment in this parameter at same Reynolds number for test of 20PPI when contrasted with 10PPI. Based on these results the it portraits the overview of the thermal properties of hollow ligaments at low Reynolds number whose application can be in electronics cooling , low flow rate of heat exchangers or solar thermal applications. The Figure 2.5 shows the Detailed cut of the 10PPI metal foam. (Beer, Rybár, & Kaľavský, 2019)

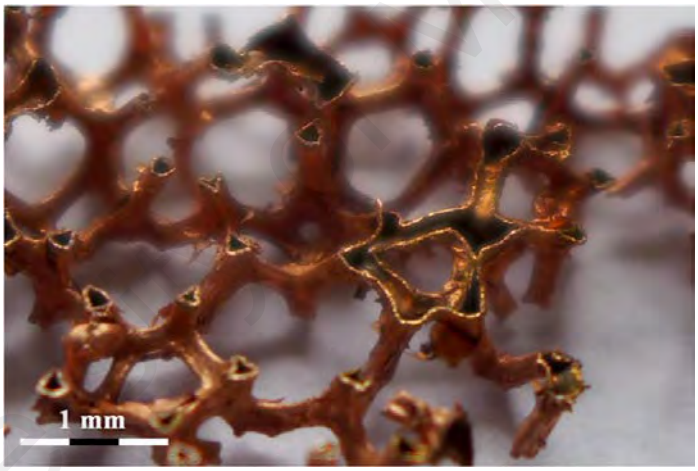

Figure 2.5: Detailed view of Hollow ligament after machining 10PPI foam

The study possess the application for the compact heat exchangers. The metal foams were identified with average pore diameter 2.3mm that was subjected to forced convection and water was used as the coolant. The experiments performed scaled to estimate the heat exchanger performance when used with 50% water – ethylene glycol solution and were compared to commercially available heat exchangers. These metal foam generated thermal resistance that were two or three times lower than the market one. The compressed aluminum foams performed well in terms of heat transfer when compared to the market one.(Boomsma, Poulikakos, & Zwick, 2003)

As (Boomsma et al., 2003) evaluated the aluminum foam property this study from (Nawaz, Bock, & Jacobi, 2017) has been done to investigate the thermal hydraulic performance of heat exchanger under dry operating conditions. The impact flow conditions and metal foam geometry on the heat transfer coefficient and gradient have been investigated. The metal foams with two different PPI of 5 and 40 have been compared for the study. The results show that the pore with smaller diameter have larger heat transfer coefficient. The permeability and the inertia coefficient were reviewed, and potential issues have been identified.

The studies for the metal foams have been vast and here is another application of the metal foam. This study is an investigation based on the heat transfer characteristics of the mixed convection flow through rectangular channel. The experiments were conducted with the uniform heat flux. The temperature of the surface wall has been measured for three values. The results were recorded from the Reynolds number against the Nusselt numbers and Richardson numbers for the heat transfer characteristics. The study was done in three different Aspect Ratios (AR) for 0.25, 0.5, and 0.1. The results show from the experimental data obtained that 30PPI has more heat transfer when compared to others and the use of foam has its advantages.(Kopanidis, Theodorakakos, Gavaises, & Bouris, 2010)

2.3.1 Heat transfer and Pressure drop characteristics

The open cell metal foam greatly affects heat exchange and pressure drop by every change done. The accompanying examination was the analysis led in wet air with hydrophobic covering under dehumidifying conditions. The heat trasnfer and the pressure drop attributes were contemplated tentatively and was contrasted and the uncoated metal foam. The gulf air temperatures was found between 27-35˚C with the relative dampness 30-90% and speeds fluctuating between 0.5-1.0 m/s. The outcomes for the heat exchange

and the weight drop were explored for various kinds of PPI going from 5 - 40PPI. The basic thing was the when the pores was expanded the volume of the cell diminishes. As the PPI increments from 20 to 40 PPI the decrement of heat exchange coefficient with expanding PPI at high relative moistness conditions. The heat transfer exchange coefficient of wet air in metal froth with hydrophobic covering was 5 – 34% bigger than the uncoated metal foam. When the relative humidity was 30% the pressure drop was almost equal to uncoated metal foam and while the relative humidity at 70% and 90% was larger by 95 % than the uncoated metal foam.(Hu, Lai, & Ding, 2018)

(J. Wang, Kong, Xu, & Wu, 2019) in his study has explained The quick advancement of electronic gadgets has made it important to create novel and imaginative heat the board arrangements. This paper tentatively explored the warmth exchange and stream attributes of three new finned copper froth heat sinks exposed to the impingement cooling by rectangular space stream and hub fan. The impacts of warmth sink stature (H, 15, 30, 45, 60 mm), the pore thickness of the embedded copper froth (PPI, pore per inch including 10, 20, and 30) and the gas stream Reynolds number (Re, shifting from 2053 to 12737), were methodically examined. Two sorts of regular finned heat sinks, with 8 and 22 blades however without copper froth, were additionally tried for correlation. Test results uncover that embeddings copper froth decidedly improves the warm execution of finned heat sinks exposed to fly impingement. Likewise, the warm execution of finned copper froths with 20 PPI and 30 PPI even surpasses that of a customary finned heat sink with 22 blades at a low stature, for example, 15 mm, appearing incredible potential to supplant conventional finned heat sinks. Be that as it may, embeddings metal froths prompts an a lot bigger weight drop than those of ordinary finned heat sinks. From this work, finned copper froths are described by a superior warmth exchange execution than a customary warmth sink with a similar number of blades. Indeed, even with expanded stream opposition, finned copper froth heat sinks still have application prospects in some

restricted and thin spaces where siphon control utilization is not the prevailing thought. The Figure 2.6 shows the difference between the pressure drop of the coated and the uncoated foam in different velocity.

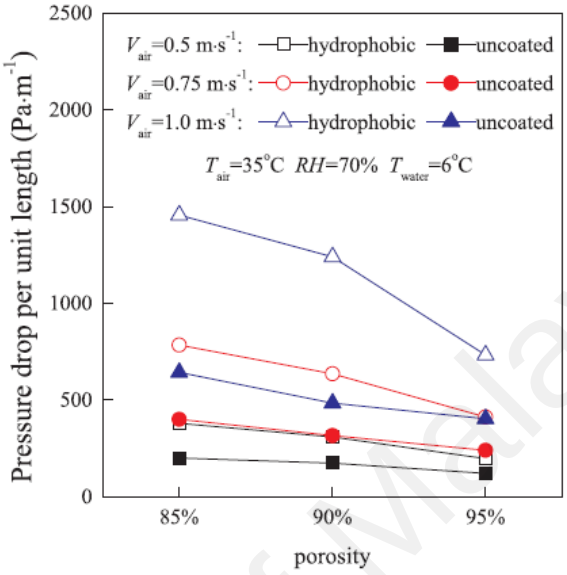

Figure 2.6: Pressure drop of coated and uncoated foam with different velocity

As mentioned earlier about the effect of heat transfer and the pressure drop in the metal foam this study is a comparison of analytical and numerical prediction of the same. The investigation built up a streamlined scientific model dependent on the jewel molded unit cells which had been created to anticipate the warmth move in a metal froth channel. The model depended on the structure of circle focused open cell tetrakaidekahedron which was fundamentally the same as genuine microstructure of an aluminum metal froth. The recreation of the stream designs and the lattice freedom were researched. The study was compared to open channels and had been found that heat transfer rate offered by the foam channel is one order of the magnitude and two orders of magnitude higher than those of microchannel and macrochannel. The Figure 2.7 shows the heat transfer coefficient compared with analytical and experimental.(M. Bai & Chung, 2011)

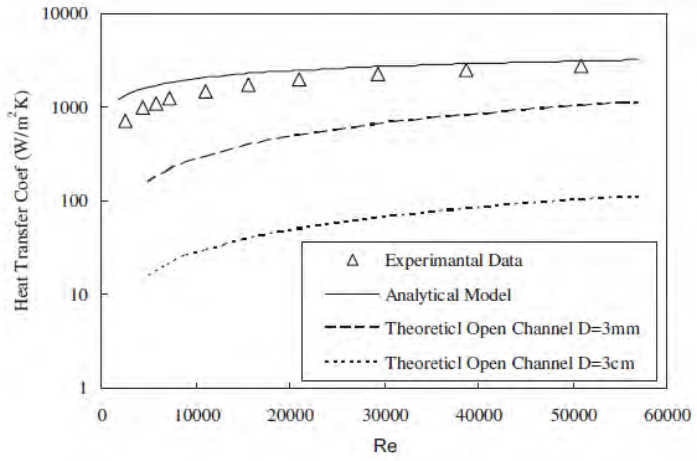

Figure 2.7: Heat transfer coefficient values compared with analytical and experimental model

The examination was the examination of warmth exchange and weight drop in metal froth filled in the pure cylinder heat exchanger under the convective limit condition. The air speed inside the cylinder was differed generally high between 7 – 26 m/s. The impeccable cylinder was fabricated utilizing the metallic sintering strategy are of various pore densities 10, 30, and 70 PPI with the porosity of 0.93. The pneumatic force drop through the hardened steel was likewise estimated. The inertial drag was the overwhelming piece of the weight drop at the higher speeds. The impact of the limit condition on the warmth execution was tended to by the examination of the Nusselt number. The 10 PPI cylinder has the biggest porousness of 3.2 × 10-8 m2 and minimal type of coefficient of 144.26 m-1. The Nusselt number got under steady warmth transition limit condition was a lot higher than the one which was gotten under convective limit condition. The Nusselt number obtained with this study increases with the pore density. The Nusselt number effect on the convective boundary condition was great.(H. Wang & Guo, 2016)

2.3.2 Heat transfer Surface Area

The heat transfer territory is the essential computation of the Heat exchanger that demonstrates the effectiveness and the execution. This investigation is apparent that heat

exchange region has more noteworthy impact in the heat exchange region or the measure of metal foam utilized. This examination is the examination of the stream and warmth qualities of twofold covered sintered woven work with porosity. The examinations were done in the packed air and the gulf Reynolds number fluctuating from 550 to 3200. The examples were warmed electrically, and the surface temperatures were estimated. This demonstrates the penetrability increments with normal porosity and the inactivity coefficient had negative propensity. The pressure drop curves of the same porosity combination coincide nearly and the pressure drop is linear.

$$S = \frac{6\,V\,(1-\varepsilon)}{dp} \qquad \textbf{Equation 3}$$

Where S is the total heat transfer area of the woven wire mesh, V is the total volume of wire mesh , ε is the porosity of the porous medium, d_p is the average spherical diameter of the porous medium. The results show that the heat transfer and the pressure drop increase with the increase in Reynolds number for the same test piece. The average porosity has also a great influence.(Ma et al., 2016)

2.4 Past research

The metal foam impact were considered for the cooling execution of copper metal foam heat sink under lightness initiated convection. This work was the examination of copper metal foam with porosity 61.3% with the 20 Pores Per Inch. The pressure drop try is completed independently to ascertain the penetrability and the warmth exchange coefficient of the permeable media. The pressure drop is extraordinarily influenced by the tendency of the permeable media from level to vertical position. The Hazen – Dupuit model was utilized to bend fit the longitudinal worldwide weight drop against the normal liquid speed information. Two distinctive metal foam of aluminum and copper were researched for the investigations. The results show that the heat transfer increase in different Reynolds number and had been varied with the heat flux supplied to it.

$$h = \frac{Q}{Ab\,(Tb - Tamb)} \qquad \textbf{Equation 4}$$

where h is the heat transfer coefficient, Q is the heat flux varied, A_b is the area of the block of copper and aluminium foam, T_b is the temperature at the surface, T_{amb} is the inlet fluid ambient temperature. The Figure 2.8 and Figure 2.9 shows the heat transfer coefficient in copper and aluminum block.

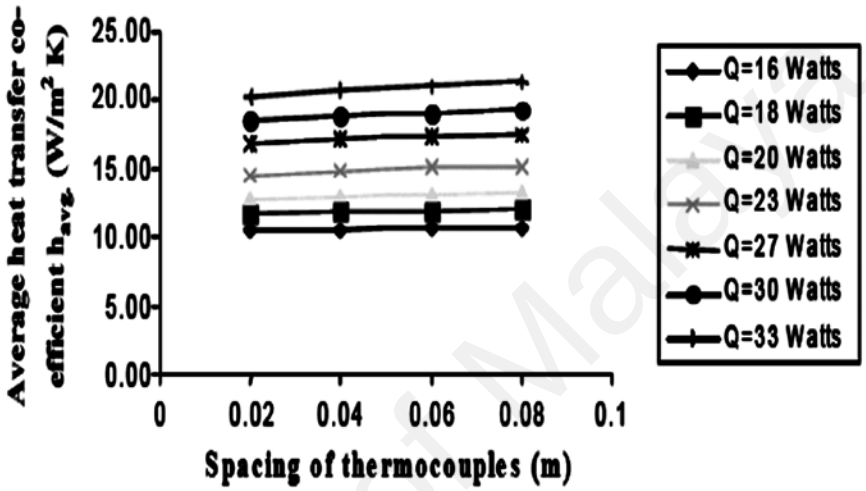

Figure 2.8: Heat transfer coefficient in Copper block

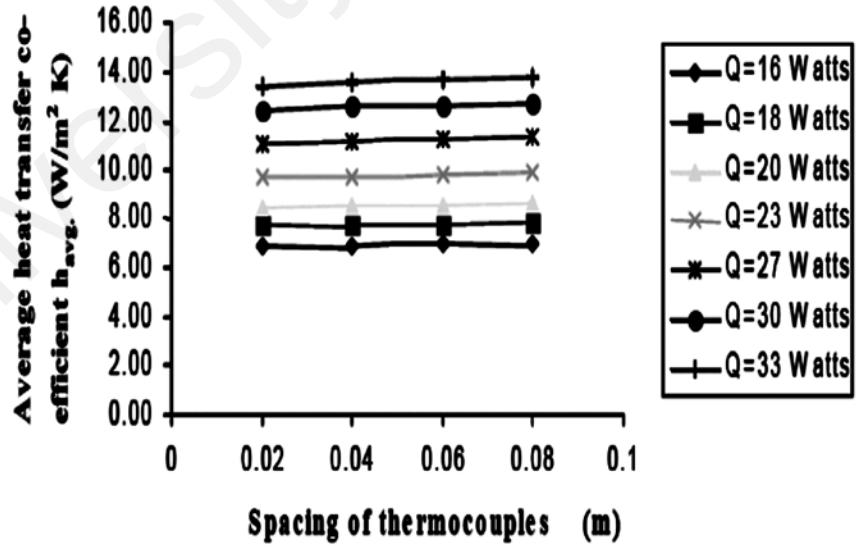

Figure 2.9: Heat transfer coefficient in Aluminum block

The above figures are the heat transfer coefficient of different metal foam of copper and aluminum. The final results of comparison of the aluminum and copper have been

made and the results show that copper metal foam has large accessible surface area and high cell wall conduction.(P. Elayiaraja, July 2010)

2.5 Research gap

The previous study show that the copper metal of different porosity with different number of Pores Per Inch have been investigated for the heat transfer and the pressure drop. It is clear from this examination that the copper metal froths have more noteworthy impact on porosity. The tried example results demonstrate that the warmth exchange coefficient does not rely upon the heat motion. The essential target was set to look at the worldwide and interstitial heat transfer coefficient. The results show that the copper with the 10PPI shows the best heat transfer performance.(Mancin, Zilio, Diani, & Rossetto, 2012). Now furthermore adding (Shi, Zheng, Chen, & Dang, 2019) have conducted the test in 10 PPI hydrophobic annular metal foam partially filled in a tube. The experiment was carried to to find the average Heat Transfer Coefficient (HTC) of 10PPI foam. The average inlet water temperature was fixed to 55˚C by varying the mass flow rate. The results show that the localized heat transfer inside the tube at different rate of mass flow. It is proved that heat transfer can be increased if properly treated when compared to untreated metal foam.(Shi et al., 2019)

The main objective of this research is to develop the compact metal foam heat exchanger with different configuration. (Javadi et al., 2019) and (Tiwari et al., 2019) have developed different types of ground heat exchangers that deal with Pores Per Inch ranging from 5 – 40 PPI. As the Pressure Drop and the heat transfer coefficient of the tubes filled heat exchanger have been carried by (Shi et al., 2019) and (H. Wang & Guo, 2016) the research gap was identified. This research is aimed to carry out the development of compact heat exchanger with 60PPI (Pores Per Inch) with different designs. The uncoated copper metal foams will be used to analyze the thermal hydraulic performance with each

design. This was because to understand the behavior of the metal foams with higher porosity and number of pores. The heat transfer and pressure drop of each developed heat exchanger will be analyzed and studied at each localized point to estimate the overall performance.

CHAPTER 3: RESEARCH METHODOLOGY

The research methodology chapter will clearly describe the design and the development of the wind tunnel for the heat exchanger in detail. The measurements and the instruments used to record the data are also elucidated in detail.

3.1 Development of wind tunnel

The open forced convection wind tunnel is a system which grips the heat exchanger inside the test rig. It was initially designed and fabricated in small scale. The wind tunnel comprises of the following parts such blower or the fan, settling chamber, test rig and the base which are assembled later to form a system. The 3D model in the solid-works software was designed. The complete solid works model (CAD) design is shown in the figure below.

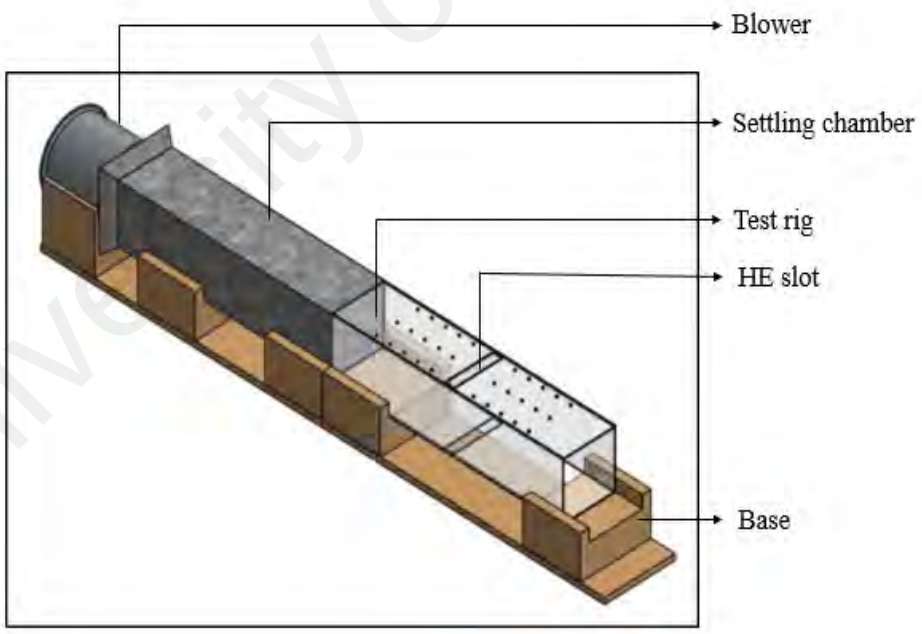

Figure 3.1: CAD 3D- Model of the developed wind tunnel

The above Figure 3.1 is the complete setup assembly of the open forced convection wind tunnel with heat exchanger. The holes in the test rig is given to analyze the velocity profile of the flow developed inside the test rig.

The axial blower or fan is mounted which is the source to give power to the air. In this research study the working fluid was set to air and incase of liquid a motor is required to drive the coolant. The length of the channel of the wind tunnel depends mainly on the flow produced which was the entry length. The settling chamber is the tunnel where the working fluid (air) enters before going to the test rig. The purpose of the settling chamber is to provide length for the fluid to get fully developed where the velocity profile will be flat. If the settling chamber is not placed the velocity profile seems to be distorted and does not follow any regular pattern.

The test rig is the main assembly of the system in the wind tunnel with the dimensions of 230mm height 230mm width and length of 1000mm with the thickness of 5mm. This section is the place where the different configuration of heat exchanger is placed. The test rig is given provided with holes on top of it with a diameter of 8mm before and after the HE. The holes are provided mainly to measure velocity profile of the developed wind tunnel and to see the air flow developed inside the test section. The velocity profile is recorded by the manometer and the pitot tubes. To hold all the above components together and fix it rigid, the base was fabricated. It serves another main purpose such as to reduce the vibrations produced by the axial blower. To bring all the sub-assemblies like blower, settling chamber and test rig in line the base is necessary.

3.2 Development of heat exchanger

The heat exchanger is basically a device which is used to transfer heat from the one form to another. There are different working fluids used to carry out the heat such as refrigerants in the form of gas and liquid, water and air. The working fluid used to carry out the research was set to air which is from the source of axial blower. The HE can be in any form of design and basically the main aim was heat transfer and keeping that in mind

it was developed. The open cell copper foam with varying PPI is used to carry out the research and to arrive at the objectives.

3.2.1 Open cell metal foam

The cellular structures that are interconnected together to form like honeycomb in a large volume is known as open cell metal foam. There are other different types of metal foams available, the metal used in my research was copper metal foam. Initially the metal foam will be large square shaped sheets as shown earlier. Later which is machined in a W-EDM (Wire – Electric Discharge Machining) machine to cut it for the required size which can fit in the heat exchanger. After machining, the separate strips is shown in the below Figure 3.2.

Figure 3.2: Multiple strips of Copper after machining

3.2.2 Heat exchanger housing

The heat exchanger housing is developed to hold the metal foams and the fins together to carry out the experiment. The material chosen for this housing was aluminum which has high thermal conductivity when compared to stainless steel. The heat flux produced

by the cartridge heaters should be conductive heat transfer and aluminum is supposed to do this. The heat flux in the stainless steel will not be uniform and also cost wise aluminum is considered to be cheaper than the stainless steel. The dimensions of the housing are with 240mm x 200mm x 32mm respectively. Two holes above and below the housing alongside of diameter 13mm are drilled for the cartridge heaters to be placed inside as shown in Figure 3.3.

Figure 3.3: Aluminium Heat exchanger housing

3.2.2.1 Temperature Interface Material

The thermal connection between two surfaces which are to be mated for enhanced heat conduction which are a category of products are known as temperature interface material. This TIM (Temperature Interface Material) can also be Phase Change Materials (PCM) and are available in many forms such as creases, gels, putties, thermal pads and adhesives etc. The TIM material used in my research is PCM which is paper form of thickness 0.05mm and is placed in between the metal and the aluminum housing to enhance the heat conductance.

3.2.3 Cartridge Tube Heaters

Omegalux Cartridge heaters are heavy industrial joule heating element for producing heat at various temperatures which can customized for the design from the manufacturers. In this research two cartridge heaters each of diameter 12.5mm and 600W are used one at the top and the other at the bottom to produce constant heat flux to the element. The maximum service temperature of this heater is up to 450°C and the accuracy of ±1˚C where the lead wires are used in this. The heater is surrounded by the stainless steel to avoid oxidation and a TIG (Tungsten Inert Gas) weld is done to seal the instrument. The length of the heater rod used in this 200mm with a tolerance of ±5mm with the housing to fit in. The below Figure 3.4 shows the cartridge heaters of different sizes available in the market.

Figure 3.4: Cartridge Heaters of different size

3.2.4 Insulation

Insulation, that acts as a barrier to prevent the heat dissipating to the surrounding and keeping the place intact without change in temperature. The test section was completely wrapped inside with the ceramic fibre blanket which is a type of refractory wool. The maximum service temperature of this wool is 1200°C. It can offer low thermal

conductivity and low heat capacity. The below Figure 3.5 shows the insulation wrapped around the test rig.

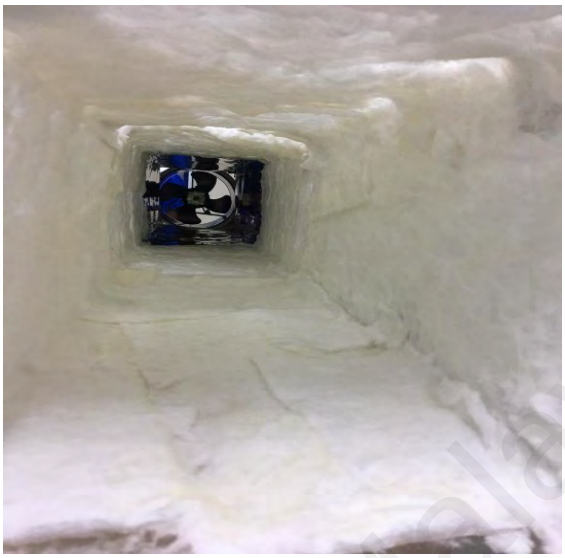

Figure 3.5: Insulation draped around the test section

3.3 Different configuration

As mentioned in earlier chapter the aspiration of achieving the results with the different orientation of holding the foam in different axis. The foam arrangements also play a significant role as like the PPI of the foam to be used depends. When the arrangement is modified the heat to be transferred also vary with PPI. In this research the densely packed pores of 60PPI are chosen for both design. The effect of this arrangement and the analysis of this study will be explained in following chapters.

3.3.1 Design 1

The complete Design-1 housing heat exchanger is shown in Figure. The heat exchanger is arranged with copper foam and aluminum fins consecutively which is closely packed. The copper strips metal foam has a purity of 99.9% without any composition. Each copper foam has porosity (ε) of 0.93 on average. The foams used in this design is 60PPI with average pore diameter (d_h) 0.556mm and the spherical diameter (d_p) was found to be 0.062mm. The thermal conductivity of copper (K_c) and aluminum

(K_{Al}) are 401 W/m-k and 237 W/m-k respectively. In this design the total number of aluminum fins were 28 and total number of copper strips were 29. The length and width for the fins and foams are 200mm and 20mm respectively. The thickness for the copper metal foam is 20mm and for the aluminum fins is 2mm. The Figure 3.6 shows Design 1 of the metal foam.

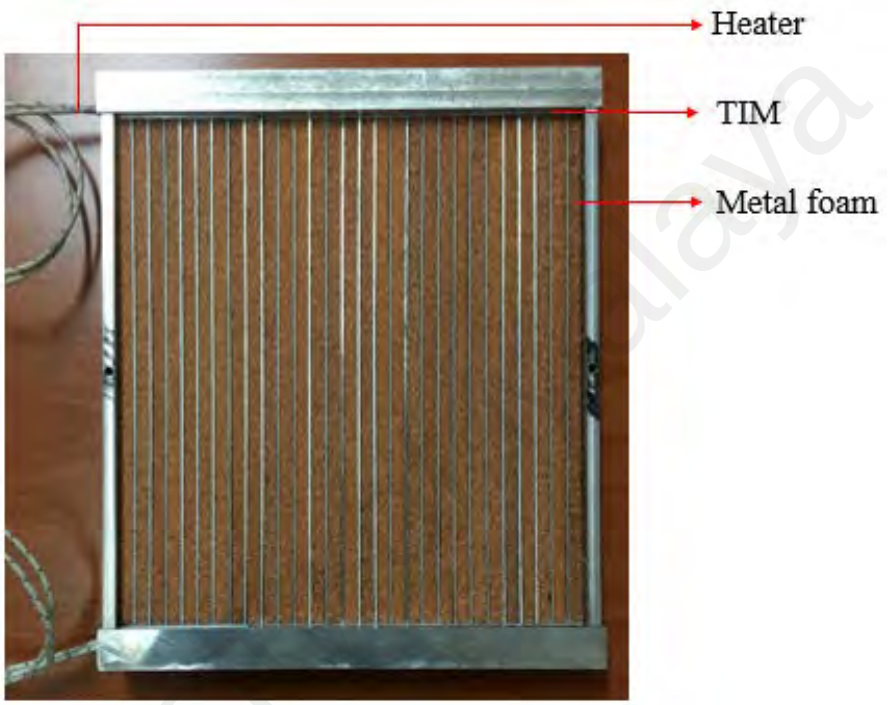

Figure 3.6: Design-1 Cofiguration – Closely packed

3.3.2 Design 2

The completed Design 2 housing heat exchanger is shown in the figure. The purpose of the design 2 was fabricated to see the after effects of the air gap in between the metal foam and the aluminium fin. Two aluminium fins with one metal foam was one pair. Each pair of aluminium fin and foam were mounted with air gap of 5mm in between. The copper strips metal foam has a purity of 99.9% without any composition. Each copper foam has porosity (ε) of 0.93 on average. The foams used in this design 2 is 60PPI with average pore diameter (d_h) 0.556mm and the spherical diameter (d_p) was found to be 0.062mm. The thermal conductivity of copper and aluminum are 401 W/m-k and 237

W/m-k respectively. In this design the total number of aluminum fins were 28 and total number of copper strips were 15. The length and width for the fins and foams are 200mm and 20mm respectively. The thickness for the copper foam were 5mm and the aluminum fins were 2mm. The Figure 3.7 shows the Design 2 of the metal foam.

Figure 3.7: Design 2 Configuration – Air gap

3.4 Measurements and instrumentation

The measurements and instruments controlled are explained clearly in detail in this section.

3.4.1 Manometer and Pitot Tubes

The Testo 521-1 (OMEGA) differential pressure measuring manometer with accuracy of ±1.2˚C and pitot tubes was used to measure the pressure drop inside the test section after the insertion of the specimen. Initially the velocity profile for the test section was calculated using this instrument to track the flow of air from the blower in the entrance region. The Pitot tubes connected with the manometer to get the differential pressure,

absolute pressure, relative pressure and temperature after which the series of data were recorded using the data cable. The Figure 3.8 shows the instrument.

Figure 3.8: Manometer with Pitot tubes

3.4.2 Temperature controller

The temperature controller is the central component which is the source for the supply of heat to the heat exchanger. The experiments were all conducted in steady state condition which were maintained at a temperature of 50˚C for all the measurements. The SR1 series digital controller coupled with Celduc heater and heat sink is connected to the cartridge tube heaters. The heat supplied to the heaters are maintained constant for all the measurements. The Resistance Temperature Detector (RTD) sensor is mounted in the middle of the housing to countercheck for the stabilizing the heat. The time taken to stabilize for the heat exchanger with heat given as input and the RTD temperature output is around 15-20min. The Figure 3.9 shows the heater.

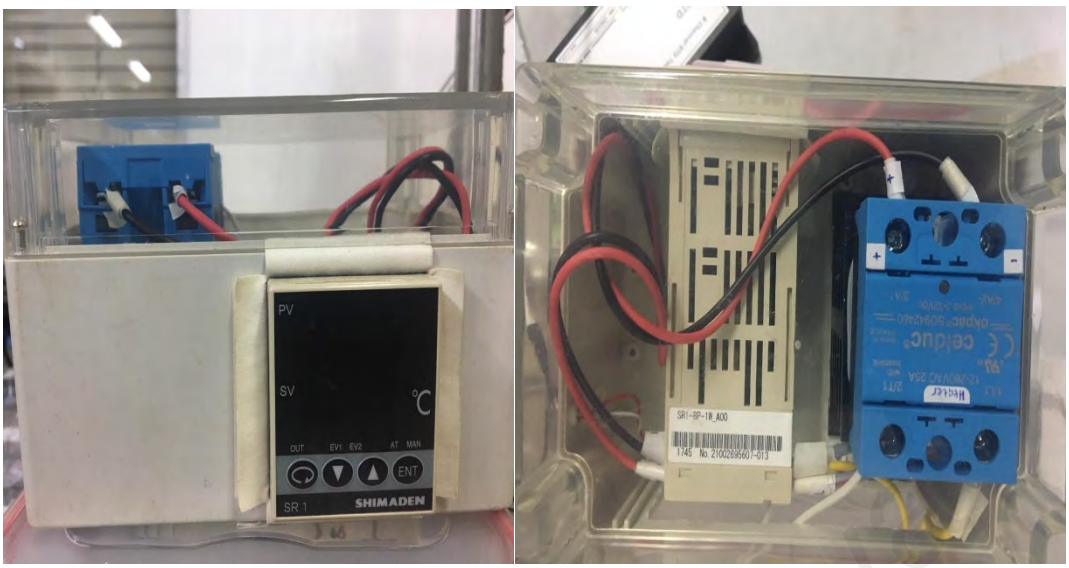

Figure 3.9: Temperature controller with Heat sink coupled

3.4.3 The 8-channel data logger

Omega 8- channel data logger is used to record the temperatures at all the required points. The software encrypted with the device allows to measure all the temperatures and covert it to data. The device can measure up to 500,000 readings and save it to the memory. The accuracy is ±0.1˚C and the temperature range is -20˚C to 60˚C. The Figure 3.10 shows the Data Logger

Figure 3.10: Omega 8-channel Data logger

3.4.3.1 Thermocouple

The thermocouples are the devices to measure the temperature at that point to know the temperature of the working fluid (air). The amount of heat transferred to the fluid is calculated by the heat transfer coefficient, (**h)** by knowing the fluid temperature. The bulk fluid inlet and exit temperature with the temperature effects on the metal foam is recorded by the thermocouple and is recorded by the data logger. In this K-type thermocouple are used which is the composition of nickel and chromium and the range is from -210˚C to 600˚C. The Figure 3.11 shows the thermocouple used.

Figure 3.11: K-type thermocouple

(a) ***Measurement point in the test rig***

The average inlet and exit bulk fluid temperature is recorded at the entrance region and the exit points of the test rig. For the velocity of the flow inside the test rig the anemometer is fixed at the entrance region and to see the velocity profile. The thermocouples are placed on the metal foams in the heat exchanger. For instance, at thermocouple 1 the average temperature is recorded and the heat transfer coefficient at that point is calculated which is $\mathbf{h_1}$. Similarly, for the remaining points h_2, h_3, h_4, h_5 and h_6 the temperature at each point is recorded and the heat transfer coefficient is calculated locally. The distance between two thermocouples is 40mm from the bottom.

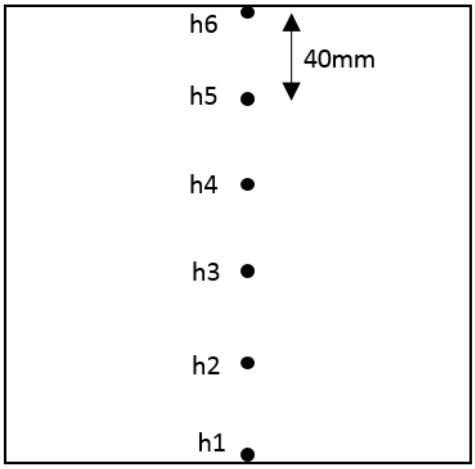

Figure 3.12: Placement of thermocouples with spacing

The velocity profile for the test section was measured inside the test section to see the effect of air flowing inside. The Figure 3.13 below shows the points of the velocity measured using the manometer mounted with the pitot tube. The points shown are the front view of the test rig where the velocity is locally measured at that point. Two regions that is the region before the specimen and the region after the specimen were recorded.

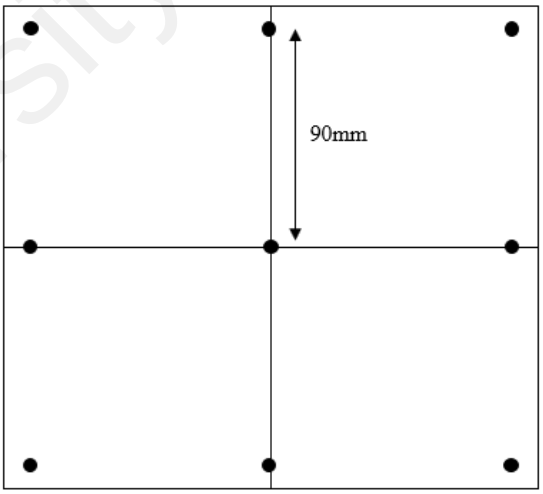

Figure 3.13: Velocity Profile measurement points in test rig

3.5 Experimental Calculation

This section explains about the calculation for the parameters conducted experimentally in detail.

3.5.1 Pressure Drop of the developed design

The properties air at the ambient temperature corresponding to 1atm pressure were referred as density, $\rho = 1.184 Kg/m^3$ and kinematic viscosity, $\nu = 1.562 \times 10^{-5} m^2/s$.(Yunus A.cengel, 2016) .

$$Re = \frac{v \times Dh}{\nu} \qquad \textbf{Equation 5}$$

Where Re- Reynolds number, v- velocity (m/s), Dh- Hydraulic meter (m), ν- Kinematic viscosity.

The pressure drop difference for both Design 1 and Design 2 were recorded from the 130mm from the heat exchanger specimen in both the sides.

3.5.2 Heat transfer coefficient (h) of the specimen

The heat transfer coefficient (h) is the ratio of the heat flux (q) and the thermodynamic driving force that is the temperature difference(ΔT). The heat transfer coefficient relation is given below:

$$h = \frac{\text{Qair}}{A \times (Tw - Tamb)} \qquad \textbf{Equation 6}$$

Where h- heat transfer coefficient (W/m^2K), Q_{in} – power given as input to the heater (W), A – Total average heat transfer area of design 1 and design 2, T_w – Wall temperature of the HE at 40mm spacing, T_{amb} – Ambient temperature

The Effect of heat transfer coefficient **h**, at each localized point are studied separately for both design 1 and design 2. The velocity of the flow is varied by placing the specimen inside the test rig to see after effects. The power measurement given as input for the

cartridge heater was measured for different velocities. The temperature of the heater was maintained constant to ensure the steady state condition for both design 1 and design 2. The time taken to stabilize the for each design was also one of the factors to determine steady state region.

3.5.2.1 Input power Measurement

The Input power for the design 1 and 2 are measured using the equation below. The Q_{air} is the heat absorbed by the fluid from the heater or the heat transferred to the fluid by the heater. The power required to the necessary heat transfer is given by

$$\boldsymbol{Qair = \dot{m} \times Cp \times \Delta T} \qquad \textbf{Equation 7}$$

Where the Q_{air} is the power transferred to the fluid, $\dot{m}$ is mass flow rate of the fluid , Cp is specific heat capacity of the fluid, ΔT is the temperature difference of the bulk fluid. The input power for the fluid is required to determine the heat transfer coefficient for the each localized point for two types of design. The other form of the input power measurement can be the multimeter measured heat that is directly the voltage and the current measurement. The following equation is given by

$$\boldsymbol{Qin = V \times I} \qquad \textbf{Equation 8}$$

Where the Qin is the input power from the heater, V is the voltage , I is the current drawn by the heater. The above two equations can be used to evaluate the heat transfer coefficient for each localized point of the two design.

3.5.2.2 Heat transfer area of the Metal Foam

The heat transfer area for both design 1 and design 2 vary with the amount of metal foams used for the heat transfer. The number of metal foams differ for both the designs. The formula and the method of calculation of are similar.

$$A = \frac{6\,V\,(1-\varepsilon)}{dp}$$ **Equation 9**

Where A- total heat transfer area through metal foam, V- Total volume of the foam used, ε– Porosity of the foam used (60PPI), dp- spherical diameter of the pore, and where dp is given by,

$$dp = \frac{3\,dh\,(1-\varepsilon)}{2\varepsilon}$$ **Equation 10**

Where,dh – avg. pore size

The specification of the 60PPI used were the values taken to calculate the total heat transfer area of the foam. The details of the 60PPI foam used are

ε – average porosity of the pore = **0.93**

dh – average pore size = **0.556mm**

The total number of copper metal foams used for this design were 29. Based on the number of foams the total heat transfer area was calculated and found to be was found to be, **A_1 = 3.9 m^2.**The total number of copper metal foams used for this design were 15. Based on the number of foams the total heat transfer area was calculated and found to be ,**A_2 = 2.032m^2.**

3.5.3 Bulk Fluid Temperature (T_b)

The calculations of the heat transfer area that is for metal foams used was done by the above method. The results show that the heat transfer area for design 1 is much higher than amount of the foams used in the design 2. Also, the configuration is also one of the primary objectives. The experiments was conducted based on the heat transfer area by reducing the number of copper strips used for design 2.

The Bulk fluid temperature T_b and the Temperature Difference ΔT were evaluated for both the design 1 and design 2. The temperature difference is the difference in temperatures of outlet and inlet of the fluid in the test section and is given by the below equation.

Bulk fluid Temperature:

$$\boldsymbol{Tb = \frac{Tout+Tin}{2}} \qquad \textbf{Equation 11}$$

Temperature Difference:

$$\boldsymbol{\Delta T = Tout - Tin} \qquad \textbf{Equation 12}$$

3.5.4 Nusselt Number Correlation

The Nusselt number is non - dimensional parameter used for the heat transfer between the fluid and the solid body. The Nusselt number was evaluated for Both Design 1 and Design 2 based on the total average heat transfer coefficient of the calculation. The Nusselt number for the design was evaluated using the formula given below.

$$\boldsymbol{Nu = \frac{h\,Dh}{kf}} \qquad \textbf{Equation 13}$$

Where h is the total average heat transfer coefficient of the design, D_h is the hydraulic diameter, K_f is the thermal conductivity of the fluid at the inlet temperature. The Nusselt number relation above is the common that shows the increase in heat transfer of the design in the test section. The evaluated Nusselt number for the design are tabulated for the steady state conditions by giving constant heat flux throughout the experiment.

$$\boldsymbol{Nu = 0.023 \times Re^{0.8} \times \mathrm{Pr}^{0.4}} \qquad \textbf{Equation 14}$$

Where Pr is the Prandtl number of the fluid. The above Dittus – Boelter mathematical modelling equation for the empty channel.

3.6 Experimental setup

The schematic diagram in the below Figure 3.14 of the experimental setup is clearly shown . The axial blower with variable 5 different speed is placed at one end of the test section. An anemometer is fixed at the entrance region to record the inlet velocity of the flow for different speed. The inlet air entering the test section is the cold air. The heat exchanger with different configuration is placed at the center. The compact heat exchanger has two cartridge heaters top and bottom within the aluminum housing. The source supply for the heaters will go from the temperature controller coupled with heat sink. The temperature controller can supply heat at different temperatures maintaining the input power constant. All the experiments for both Design1 and Design2 were maintained at constant temperature 50˚C. Since one of the parameters had been constant throughout the conduct it is said to be in steady state condition. The thermocouples were mounted on the heat exchanger as shown in Figure 3.13 with a gap of 40mm between each other. The temperatures measures are recorded by the data logger and send it to the laptop. The manometer was used to measure the pressure drop of the with the effect of the velocity. Simultaneously the temperatures for inlet and outlet were recorded with the thermocouple.

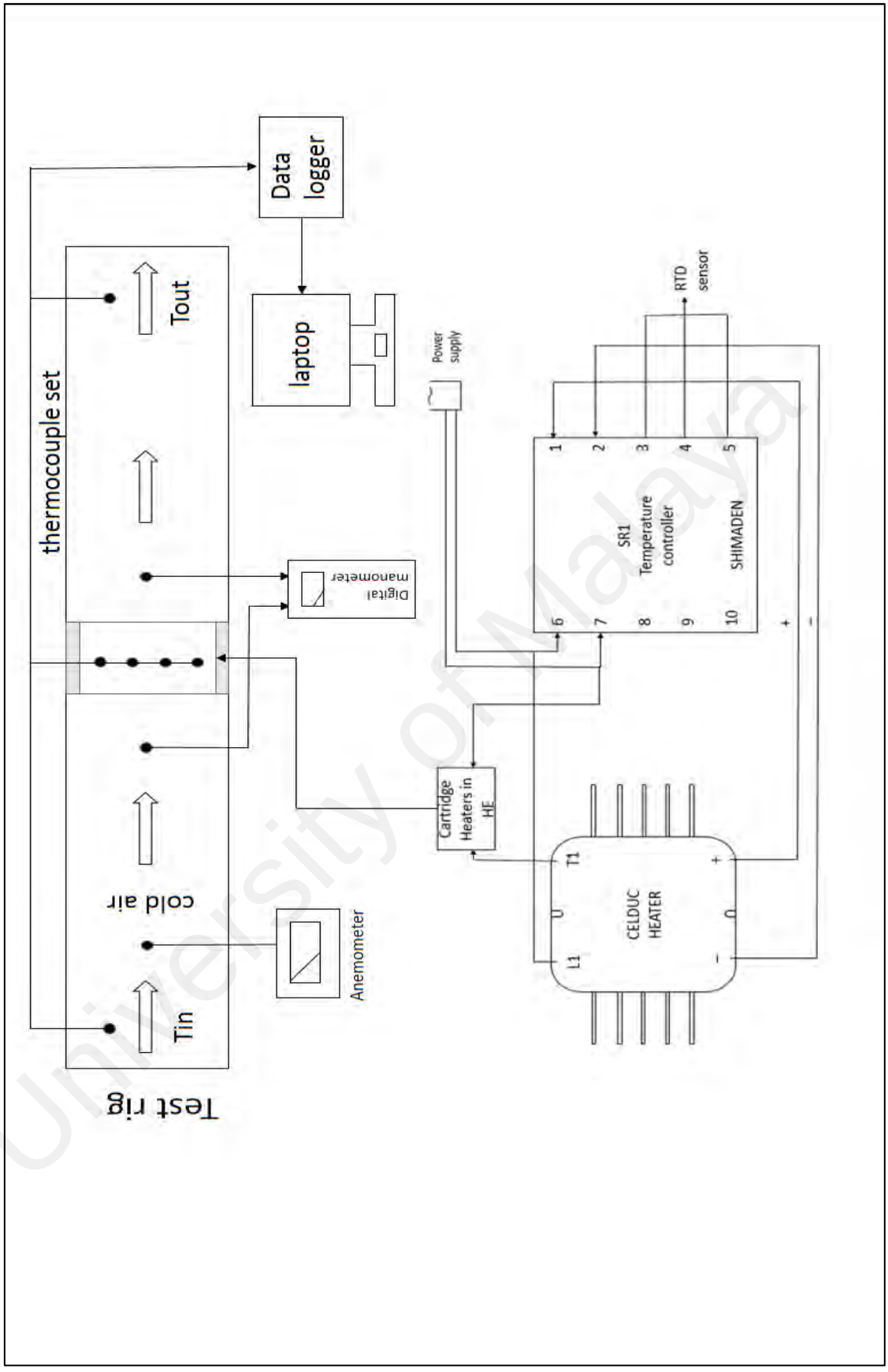

Figure 3.14: Schematic diagram of experimental setup

CHAPTER 4: RESULTS AND DISCUSSION

4.1 Experimental Provisos

The experiments for the Design 1and Design 2 metal foam was conducted with the following conditions. Assuming the flow of the fluid to be fully developed, the properties of air are evaluated at the inlet temperature and the room temperature was recorded as 22.8˚C with working fluid (air) is flowing at 1atm pressure. The experiments were carried out in steady state condition maintaining the input temperature as constant.

4.1.1 Velocity Profile of the test section

Table 4.1: Velocity Profile (v_1) - Design 1

Velocity Profile - Design 1 (m/s)							
Before				After			
	1.6	1.4	1.7		1.8	0.8	1.4
A	1.9	1.7	1.3	**C**	0.8	0.8	1.1
	1.5	1.3	0.8		1.3	0.9	0.9
	0.9	0.9	1.3		1	0.8	0.9
B	1.8	1.4	1.5	**D**	0.8	1.8	0.9
	1.7	1.4	1.6		1.8	1.9	0.9

Table 4.2: Velocity Profile (v_2) - Design 2

Velocity Profile - Design 2 (m/s)							
Before				After			
	2.9	1.4	2.2		1.4	1.3	1.9
A	2.3	1.6	1.2	**C**	2.1	1.2	1.7
	2.5	2.7	2.9		2.2	3	1.9
	2.3	1.1	2.1		1.1	2.6	2.1
B	2.8	0.9	2.8	**D**	1.5	1.1	0.9
	2.5	2.9	2.3		2.8	2.7	1.5

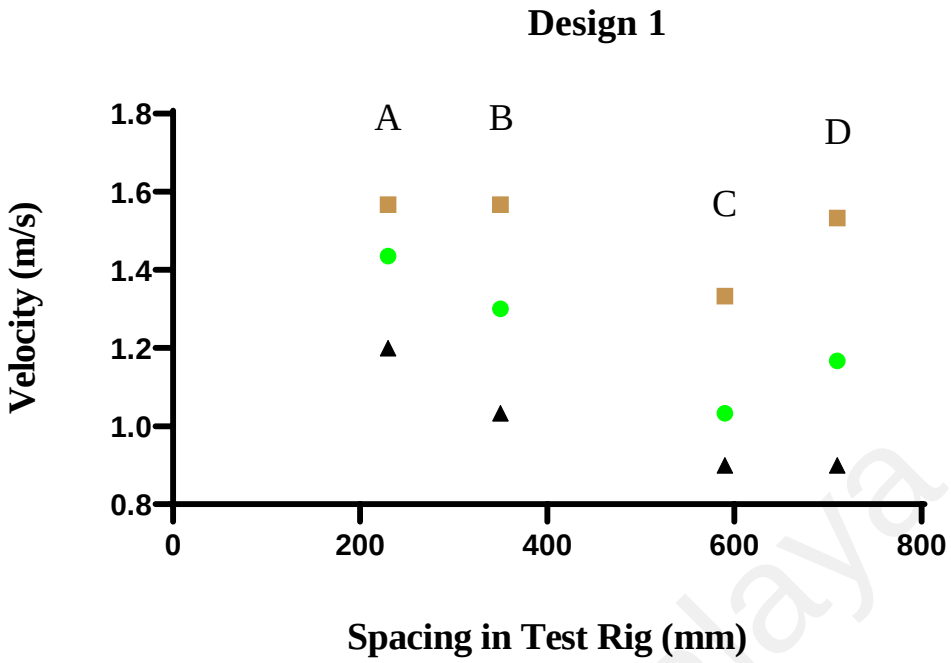

Figure 4.1: Velocity Profile (v_1) – Design 1

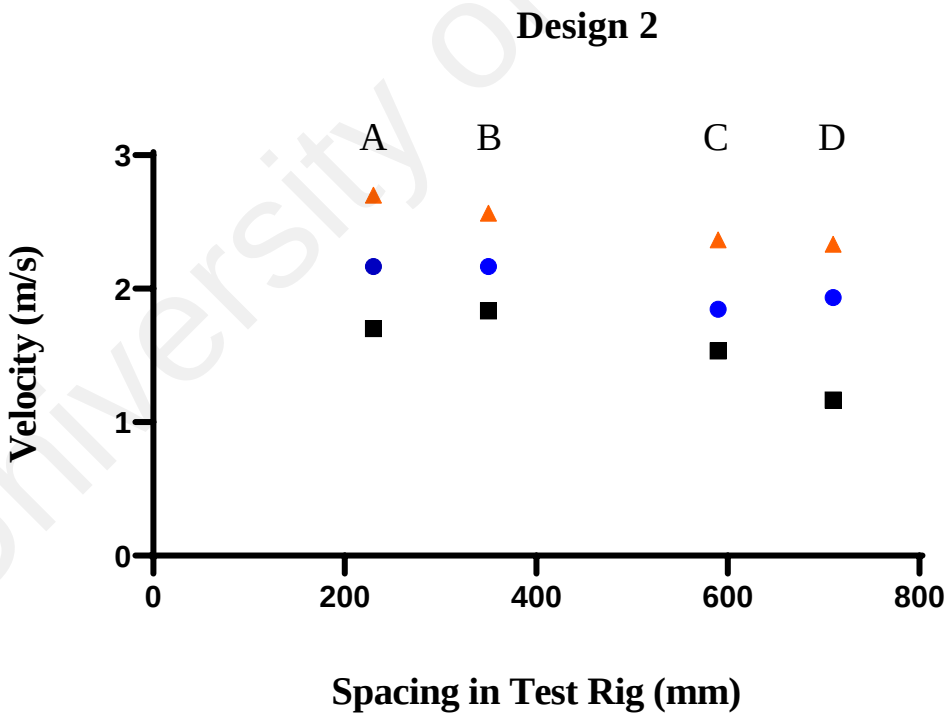

Figure 4.2: Velocity Profile (v_2) – Design 2

The Velocity Profile readings are tabulated in the Table 4.1 and 4.2 for Design 1 and Design 2. The velocity was recorded at selected localized point for each section when the specimen is inside. As shown in the Figure 4.1 and 4.2 measurement testing the velocity profile was read at these points in the two regions A and B before the specimen that is the inlet velocity and the two regions after the specimen C and D that is the outlet velocity. The velocity profile for each Design was measured and plotted in the graph to see the profile build up inside the test section. The point A is 230mm from the edge of the test section and the average of velocity in the top, center and bottom was measured. Similarly point B was located at 350mm, point C located at 590mm and point D located at 710mm respectively. The design 1 had the compact closed metal foams together that is where the velocity profile was minimum for the design 1 whereas the design 2 has the air gap of 5mm in between the foams that the fluid can pass easily and also velocity also is much higher for this velocity. This clearly shows that the velocity profile is not flat for both the design 1 and 2.

4.2 Effect of pressure drop in the test section

The pressure drop was measured inside the test section with the specimen. The effects of pressure drop and the inlet velocity passing through the test section with the Reynolds number is given below. The pressure drop pattern is plotted in the graph form to study the characteristics in both the design 1 and 2.

Table 4.3: Effect of Pressure drop in the test section

No.	Velocity – Design 1(v_1) (m/s)	Velocity – Design -2(v_2) (m/s)	Reynolds number-Design 1 (Re_1)	Reynolds number-Design 2 (Re_2)	Pressure drop(P_1) Pascal Design-1	Pressure drop(P_2) Pascal Design-2
1	0.8	1.2	11779.76	1.2	17.23	17669.65
2	1	1.8	14724.71	1.8	25.85	26504.48
3	1.1	1.9	16197.18	1.9	38.78	27976.95
4	1.3	2	19142.12	2	47.4	29449.42
5	1.4	2.3	20164.59	2.3	56.01	33866.83

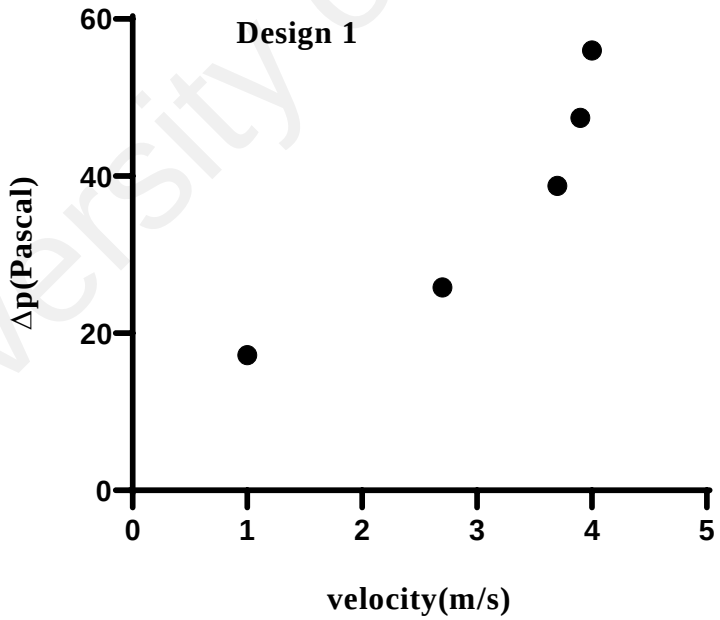

(a)

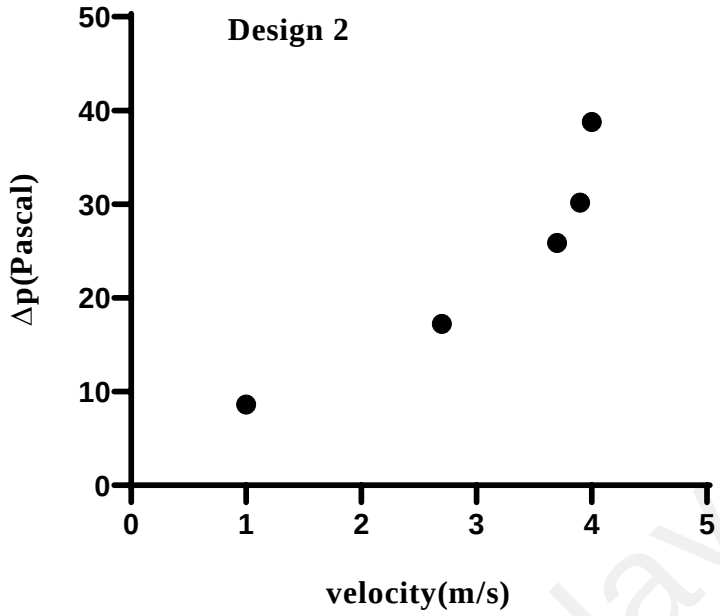

(b)

Figure 4.3: Pressure drop vs Velocity (a) Design 1 (b) Design 2

The above table shows the effect of flow of the working fluid inside the test section with the Reynolds number and the pressure drop. The axial blower is varied with 5 differential speed and each time the velocity of the speed is recorded. The pressure drop Δp , is the pressure difference between two points in the test section with the specimen. Figure 4.3 above shows the graph plotted against velocity and pressure drop. It shows clearly at the lower velocity the pressure difference is minimal inside the test section and at higher velocity the pressure difference is higher. The physics of flow through the test section complied with pressure drop relation. The pressure drops in solid porous media increase quadratically with the velocity.

4.3 Effect of heat transfer coefficient (h)

The heat transfer is based on the power input fed into the heater and below is the table for power consumption for the heater in design.

Table 4.4: Input Power measurement (Q_{in})

Velocity(m/s) Design 1	Velocity(m/s) Design 2	Input power, (Q_{in}) W Design 1	Input power (Q_{in}) W Design 2
0.8	1.2	548.311	263.18
1	1.8	767.11	444.177
1.1	1.9	874.629	494.97
1.3	2	1069.43	548.4122
1.4	2.3	1197.66	693.752

The above Table 4.4 is the values showing the power measurement of the cartridge heaters used for the Design 1 and Design 2 at different velocities. The measurement values were obtained from the multimeter with the voltage supply and current to the heater. The values show that the design 1 has consumed more power than the design 2. This is because the metal foams are densely packed together with no air gaps. The power required to stabilize the HE to 50˚C was high. The design 2 had metal foams with air gaps in between where the heat transfer area is also less when compared to design 1.

4.3.1 Calculation of heat transfer coefficient(h_1)- Design 1

The below tabulated values are the values for each localized point on the compact heat exchanger for design 1. The effect of heat transfer at each point locally was investigated to see the average heat transfer for the design 1.

Table 4.5: h_{11} - Design 1 for Velocity 0.8m/s

Inlet velocity, V= 0.8m/s						
No.	**channel 1**	**channel 2**	**channel 3**	**channel 4**	**channel 5**	**channel 6**
h1	3.27569	4.12658	4.86311	5.2052	4.80658	3.7998
h2	3.29334	4.25522	5.04821	5.40949	5.1405	3.84869
h3	3.22238	4.34062	5.23232	5.61024	5.21292	3.79672
h4	3.07508	4.35541	5.39703	5.80242	5.3134	3.65081
h5	2.86048	4.2929	5.5221	5.95984	5.44932	3.40913
h6	2.61179	4.1485	5.59239	6.06002	5.33963	3.11666
h7	2.36728	3.94369	5.5835	6.08626	5.1199	2.81862
h8	2.13407	3.69494	5.50049	6.02109	4.91582	2.52048
h9	1.91595	3.41079	5.31541	5.84099	4.58703	2.24804
h10	1.72909	3.12428	5.04821	5.57686	4.15954	2.01682
Avg. **h_{11}**	2.64851	3.96929	5.31028	5.75724	5.00447	3.12258

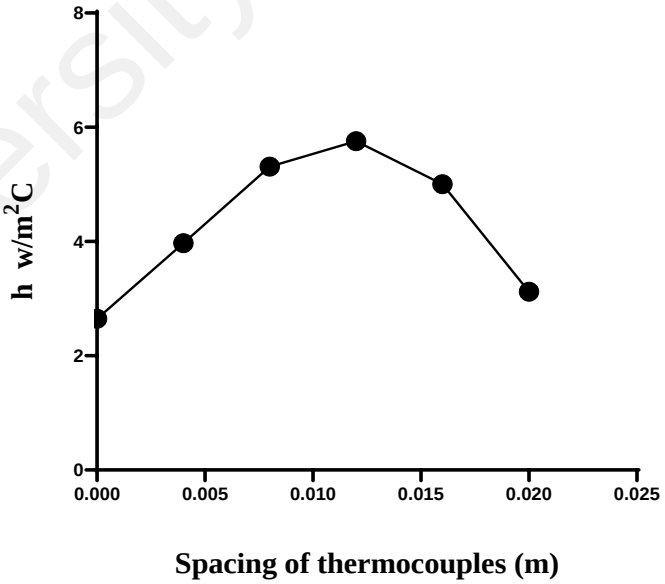

Figure 4.4: h_{11} versus spacing for Velocity 0.8m/s

The heat transfer at the localized point h_{11} are tabulated above in the Table 4.5 for the inlet velocity 0.8m/s and the results show the increase in heat transfer coefficient at the

center. This is due to flow of the inlet has more impact on the heat transfer. Since the air flow was dense at top and bottom area the heat transfer at the same was high. The Reynolds number was also one of the portion to influence the flow and it was around 11779. The average heat transfer at the top and the bottom of the HE lies in the same region where the heater was placed. The thermocouples placed in between had very gradual increase in the heat transfer coefficient. As the flow was high at the top and bottom the heat transfer follows this pattern in the Figure 4.4.

Table 4.6: h_{21} – Design 1 for Velocity 1m/s

Inlet velocity,V= 1m/s						
No.	**channel 1**	**channel 2**	**channel 3**	**channel 4**	**channel 5**	**channel 6**
h1	1.37462	3.10734	5.45012	6.67894	4.14706	1.60214
h2	1.40056	3.0434	5.15989	6.26018	3.87423	1.6062
h3	1.43962	3.02561	4.92106	5.94065	3.77751	1.62908
h4	1.48707	3.04387	4.79043	5.72953	3.7366	1.66592
h5	1.54489	3.09171	4.7203	5.60225	3.74158	1.71786
h6	1.61027	3.16077	4.70112	5.54226	3.78259	1.78004
h7	1.68101	3.25331	4.72824	5.54539	3.85525	1.84881
h8	1.68101	3.25331	4.72824	5.54539	3.85525	1.84881
h9	1.84448	3.48688	4.89778	5.6914	4.07911	2.0073
h10	1.93845	3.63308	5.03829	5.83145	4.22909	2.09741
Avg. **h_{21}**	1.6002	3.20993	4.91355	5.83674	3.90783	1.78036

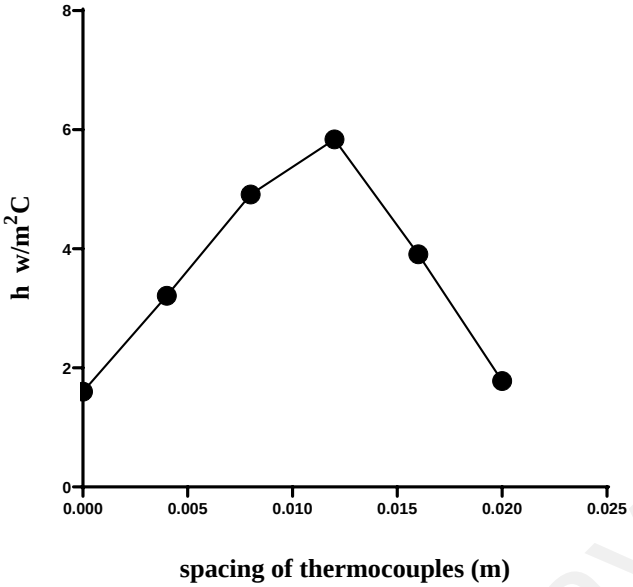

Figure 4.5: h_{21} versus spacing for Velocity 1m/s

The heat transfer coefficient values h_{21} are tabulated in Table 4.6 above for the velocity 1m/s and the results show that steep increase in the heat transfer coefficient. The heat transfer coefficient was less at this velocity when compared to lower velocity. The inlet flow velocity hitting the specimen was more at the top and the bottom and it was less at the center. The Reynolds number currently was much higher around 14724 which is two times as that of the previous flow. The heat transfer coefficient at the top and the bottom lies in the same region where as at the center it shows a very steep increase. The flow of the pattern varied with the previous velocity in the Figure 4.5.

Table 4.7: h_{31} – Design 1 for Velocity 1.1m/s

Inlet velocity, V= 1.1m/s						
No.	**channel 1**	**channel 2**	**channel 3**	**channel 4**	**channel 5**	**channel 6**
h1	1.58805	4.1592	10.1431	16.0647	10.3922	2.7396
h2	1.66454	4.29542	10.2124	16.0303	10.6135	2.86856
h3	1.75453	4.47901	10.3682	16.1109	10.9557	3.01592
h4	1.86219	4.71737	10.7664	16.6121	11.4772	3.19191
h5	1.98288	4.99585	11.2469	17.2643	12.0572	3.37849
h6	2.11151	5.28924	11.6926	17.8696	12.6346	3.55467
h7	2.2589	5.64612	12.3493	18.7668	13.3173	3.74585
h8	2.42081	6.04974	13.0919	19.7589	14.0693	3.93583
h9	2.59085	6.47226	13.8691	20.7652	14.7736	4.10965
h10	2.78002	6.95176	14.7639	21.9008	15.2457	4.27903
Avg. **h_{31}**	2.10143	5.3056	11.8504	18.1144	12.5536	3.48195

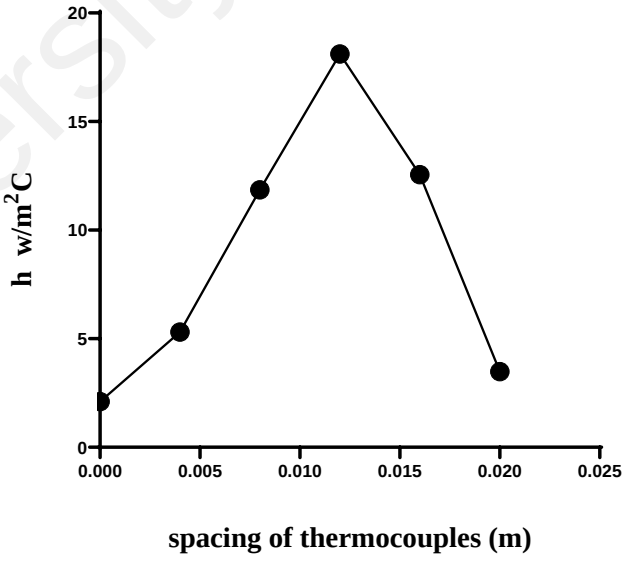

Figure 4.6: h_{31} versus spacing for Velocity 1.1m/s

The heat transfer coefficient h_{31} in the design 1 are tabulated above for the velocity 1.1m/s and the results for at this velocity show a very vertical increase. The Reynolds

number was approximately above 16197 which was much more higher than the other two velocity of the inlet flow. The heat transfer coefficient was very less at the top and bottom regions that was the heater regions and at the center it was a sudden increase of 65% more of that happened near the heater region. The effect is seen at the greater at the center which is higher than the other places. The regions near the center possess the same amount of heat transfer at this high velocity when compared to other lower velocities. The pattern of the flow shown in the graph is varies with the other lower velocities and clearly shows at the transition stage the vertical increase of the heat transfer was seen as shown in the Figure 4.6.

Table 4.8: h_{41} - Design 1 for Velocity 1.3m/s

Inlet velocity, V= 1.3m/s						
No.	**channel 1**	**channel 2**	**channel 3**	**channel 4**	**channel 5**	**channel 6**
h1	1.93407	6.34018	13.6153	20.9643	16.8332	3.38827
h2	2.02506	6.51646	13.6018	20.8844	13.962	3.5396
h3	2.13512	6.759	13.8421	21.0447	14.3642	3.71461
h4	2.25875	7.07829	14.2819	21.4062	14.8464	3.90116
h5	2.39885	7.44941	14.711	21.902	15.3966	4.09395
h6	2.56178	7.90694	15.2003	22.6248	16.1018	4.30611
h7	2.74323	8.43213	15.878	23.4972	16.9058	4.53095
h8	2.93621	9.00239	16.8126	24.571	17.7369	4.75074
h9	3.145	9.59457	17.7484	25.6754	18.4904	4.96582
h10	3.37867	10.2433	18.7946	26.8573	19.243	5.18361
Avg. **h_{41}**	2.55167	7.93227	15.4486	22.9427	16.388	4.23748

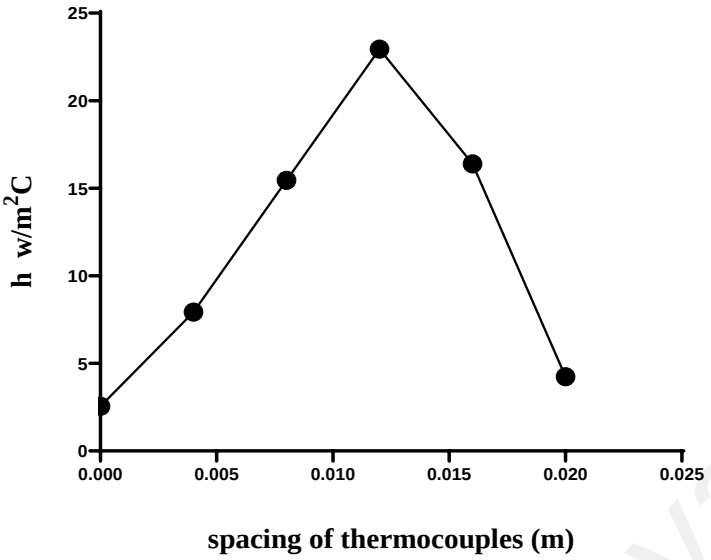

Figure 4.7: h_{41} versus spacing for Velocity 1.3m/s

The heat transfer coefficient h_{41} in the design 1 are tabulated in the Table 4.8 above for the velocity 1.3m/s and the results of the flow is shown in the above graph. The Reynolds number at this velocity was approximately above 19142 which is not much higher than the previous velocity. Although the Reynolds number lie in the same region the heat transfer flow was different. At the top and bottom regions the heat transfer coefficient was very low and at the center it increases gradually and drop. The fluid flow inside the test section when hitting the specimen is flat and seems to dense at the heater regions. Theoretically at higher velocities the heat transfer coefficient will be less that complies with the current study at this stage as shown in the Figure 4.7.

Table 4.9: h_{51} – Design 1 for Velocity 1.4m/s

Inlet velocity, V= 1.4m/s						
No.	**channel 1**	**channel 2**	**channel 3**	**channel 4**	**channel 5**	**channel 6**
h1	1.91891	4.88184	12.7009	20.633	13.3048	3.38284
h2	2.02267	5.08178	12.8618	20.7109	13.7106	3.55659
h3	2.13845	5.32555	13.2855	21.1421	14.2227	3.74608
h4	2.27506	5.62372	13.5481	21.7112	14.8705	3.94778
h5	2.42903	5.97283	14.2153	22.569	15.6425	4.16484
h6	2.59376	6.35046	15.0171	23.5174	16.3514	4.36228
h7	2.77543	6.77906	15.8964	24.6594	17.1276	4.55503
h8	2.98122	7.26969	16.8332	25.8448	17.9107	4.75569
h9	3.2038	7.81011	17.9576	27.1767	18.6921	4.94969
h10	3.41443	8.35505	18.9373	28.4453	19.4064	5.1505
Avg, **h_{51}**	2.57528	6.34501	15.1253	23.641	16.1239	4.25713

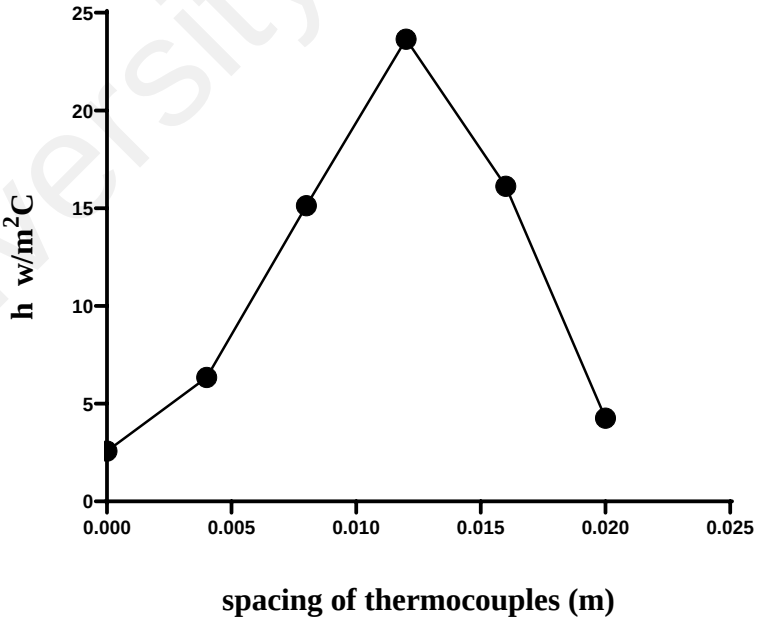

Figure 4.8: h_{51} versus spacing for Velocity 1.4m/s

The heat transfer coefficient values h_{51} for the design 1 are tabulated in the Table 4.9 above for the maximum velocity 1.4m/s and the results are plotted in the above graph.

The Reynolds number was approximately above 20164 that lies in the same region of previous one. The heat transfer characteristics was nearly same as the previous velocity as the Reynolds number of the flow lies in the same region. The heat transfer at the top and bottom show gradual increase before reaching the center and it reach peek suddenly. The bottom of the heater region shows the same pattern decreasing towards the end. As discussed earlier the velocity profile was not flat the maximum velocity hitting the specimen was dense at the top and bottom regions. The heat transfer coefficient had a gradual increase and decrease the points as shown in the Figure 4.8.

4.3.2 Calculation of heat transfer coefficient – Design 2

The heat transfer coefficient for the design 2 with air gap of 5mm is discussed below for each localized points in the heat exchanger from top to bottom with regular interval. The average heat transfer coefficient of the design 2 will be evaluated.

Table 4.10: h_{12} – Design 2 for Velocity 1.2m/s

Inlet velocity, V= 1.2m/s						
No.	**channel 1**	**channel 2**	**channel 3**	**channel 4**	**channel 5**	**channel 6**
h1	1.335785	3.736807	5.815793	5.19734	3.07351	1.208075
h2	1.306808	3.470464	5.347552	4.832751	2.951634	1.208075
h3	1.297903	3.266525	4.975709	4.570138	2.894898	1.22175
h4	1.307072	3.122414	4.701188	4.383002	2.857219	1.245363
h5	1.336474	3.04175	4.490906	4.250663	2.857219	1.277799
h6	1.382702	3.022584	4.362335	4.164557	2.874339	1.317978
h7	1.443416	3.055384	4.30864	4.124768	2.91444	1.361052
h8	1.515713	3.126182	4.310074	4.135304	2.971271	1.409487
h9	1.603537	3.233093	4.353537	4.192869	3.055384	1.464967
h10	1.703956	3.363223	4.430986	4.273102	3.151283	1.525533
Avg. $\mathbf{h_{12}}$	1.42334	3.24384	4.70967	4.41245	2.96012	1.32401

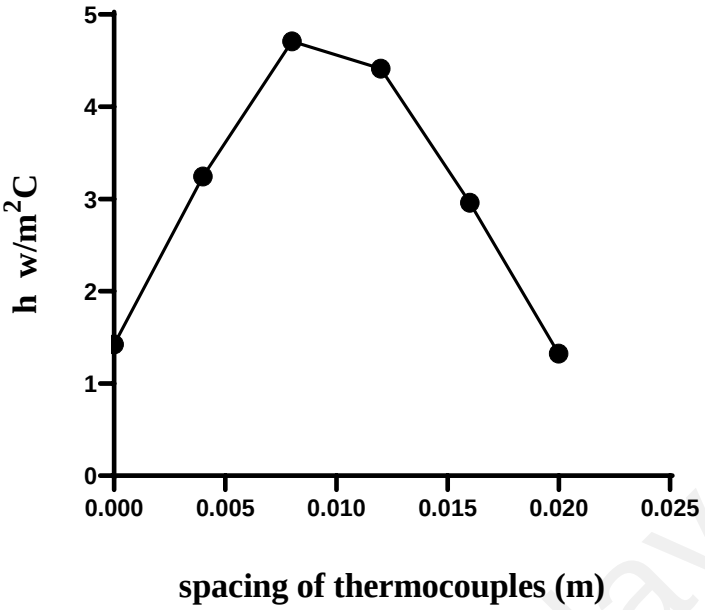

Figure 4.9: h_{12} versus spacing for Velocity -1.2m/s

The heat transfer coefficient values for the localized point h_{12} of the design 2 for the velocity 1.2m/s are tabulated above, and the results are shown in the graph. The Reynolds number for the flow was around 17669 and this is the minimum velocity. The heat transfer coefficient at the top and bottom regions were same that shows the flow at these was flat. Thereafter towards center there was gradual increase in the heat transfer coefficient after that drop crossing the center. The pattern of the flow when compared to design 1 was not same as the values differ. This is observed because the velocity of minimum can escape the air gap in between and also the heat transfer area was less.

Table 4.11: h_{22} - Design 2 for Velocity 1.8m/s

Inlet velocity,V= 1.8m/s						
No.	**channel 1**	**channel 2**	**channel 3**	**channel 4**	**channel 5**	**channel 6**
h1	2.123068	7.455356	11.57792	11.76486	7.015117	1.76625
h2	2.250963	7.726795	11.6025	11.7966	7.16457	1.827226
h3	2.405271	8.117009	11.89288	11.99731	7.36741	1.8998
h4	2.575295	8.555422	12.21179	12.19816	7.589967	1.982326
h5	2.778935	9.066406	12.61345	12.54108	7.888526	2.079641
h6	3.027577	9.715157	13.15229	12.94971	8.245607	2.188756
h7	3.293522	10.35486	13.56866	13.33685	8.599176	2.303869
h8	3.588166	11.164	14.25904	13.94965	9.047643	2.439088
h9	3.897843	12.05022	15.12741	14.57274	9.503958	2.585958
h10	4.20125	12.94204	16.03749	15.2754	9.985886	2.739236
Avg. h_{22}	3.01419	9.71473	13.2043	13.0382	8.24079	2.18121

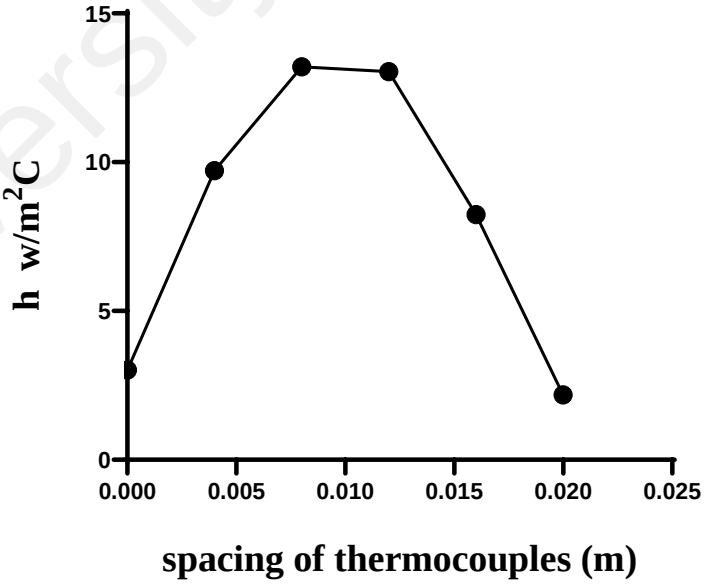

Figure 4.10: h_{22} versus spacing for Velocity 1.8m/s

The heat transfer coefficient values for the localized point h_{22} of design 2 for the velocity 1.8m/s are tabulated above and the results are plotted in the graph. The Reynolds

number was approximately above 26504 which is much higher than the lower velocity. The heat transfer coefficient was much higher at the top and bottom regions compared to other velocities in the previous design. When moving towards the center the heat transfer coefficient increase was gradual and at the center located points the amount of heat transferred was same that shows the flow was hitting the specimen was same. When compared to design 1 of this same Reynolds number its shows a steep increase. The friction was also one of the reason that the air flow can pass through aluminum fins easily inside the air gap.

Table 4.12: h_{32} – Design 2 for Velocity 1.9m/s

Inlet velocity, V= 1.9m/s						
No.	**channel 1**	**channel 2**	**channel 3**	**channel 4**	**channel 5**	**channel 6**
h1	2.478002	13.18828	21.44257	21.14476	11.62709	2.090342
h2	2.46272	12.91557	20.66053	20.53858	11.23041	2.005496
h3	2.487873	12.88823	20.13121	19.94984	11.00712	1.958415
h4	2.546389	12.90189	19.64416	19.59675	10.8165	1.948233
h5	2.619785	13.04002	19.39392	19.21038	10.68835	1.96759
h6	2.743104	13.3108	19.48701	19.24073	10.78776	2.01362
h7	2.900198	13.74648	19.66002	19.28643	10.91831	2.077683
h8	3.110158	14.28666	19.86848	19.10491	11.05207	2.158508
h9	3.428879	15.09217	20.3159	19.36308	11.37197	2.258787
h10	3.768956	15.98344	20.96279	19.90095	11.74482	2.373917
Avg. $\mathbf{h_{32}}$	2.85461	13.7354	20.1567	19.7336	11.1244	2.08526

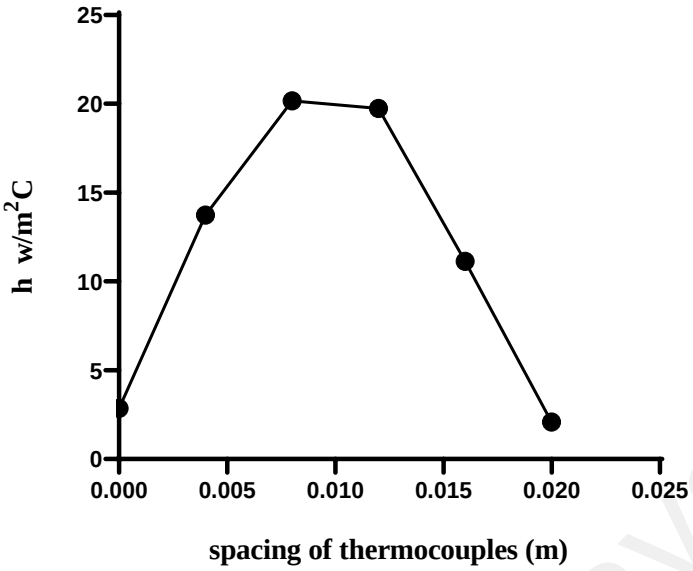

Figure 4.11: h_{32} versus spacing for Velocity 1.9m/s

The heat transfer coefficient values are tabulated above of the design 2 for the velocity 1.9m/s and the results are plotted in the graph. The Reynolds number at this stage was found to be approximately above 27976 which is much number. The transition region of the velocity hitting the specimen was much high and the heat transfer coefficient at top and bottom of the heater regions were similar. When moving towards the center the heat transfer coefficient increased 156 times within the short span of time as it was observed.

Table 4.13: h_{42} - Design 2 Velocity 2m/s

Inlet velocity, V= 2m/s						
No.	**channel 1**	**channel 2**	**channel 3**	**channel 4**	**channel 5**	**channel 6**
h1	2.598823	13.49439	23.16633	24.3581	14.15991	2.514561
h2	2.566693	13.10135	22.03166	23.12663	13.54858	2.399216
h3	2.584142	13.15243	21.71261	22.45323	12.95047	2.325015
h4	2.644922	13.44063	21.30133	21.9421	12.79696	2.298678
h5	2.724488	13.805	21.06852	21.60831	12.67079	2.315441
h6	2.829902	14.17478	21.31815	21.40268	12.58218	2.366191
h7	2.964171	14.5101	21.31815	21.47079	12.76065	2.4453
h8	3.127683	15.0523	21.57376	21.60831	13.0633	2.555272
h9	3.311913	15.7369	22.15828	21.9421	13.47418	2.690537
h10	3.508226	16.41653	22.83315	22.41593	13.9549	2.84242
Avg. h_{42}	2.8861	14.2884	21.8482	22.2328	13.1962	2.47526

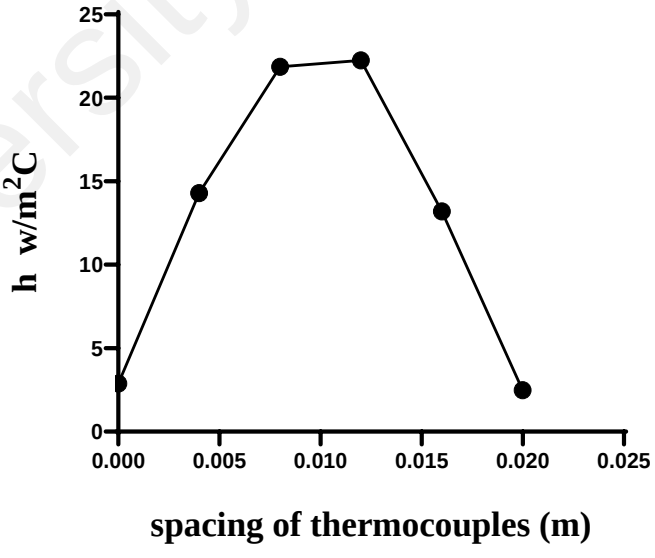

Figure 4.12: h_{42} versus spacing for Velocity 2m/s

The heat transfer coefficient values h_{42} of the design 2 for the velocity 2m/s are tabulated above and the results are plotted in the graph. The Reynolds number lies at the

same region and is approximately above 29449 which was much higher than the previous one. The heat transfer coefficient for this velocity at the top and bottom heater regions were similar that means the thermal heat transfer was equal. When moving towards the center the it is reaching a peak value which was approximately 150 times higher than the heater regions. Although air gap between the fins were provided the pattern of the flow for this design were almost similar. The effect of the velocity hitting the specimen was same from the minimum to maximum Reynolds number.

Table 4.14: h_{52} – Design 2 for Velocity 2.3m/s

Inlet velocity, V= 2.3m/s						
No.	**channel 1**	**channel 2**	**channel 3**	**channel 4**	**channel 5**	**channel 6**
h1	3.868707	22.491	36.98953	36.63234	20.07133	3.414134
h2	3.616667	20.75461	35.01676	34.94508	19.03085	3.220577
h3	3.471059	19.80356	32.89146	33.05067	18.21843	3.056521
h4	3.40834	19.159	31.61235	31.878	17.52635	2.92006
h5	3.412428	18.88348	30.429	30.7857	16.85992	2.834482
h6	3.457001	18.89393	29.63658	30.054	16.54936	2.799388
h7	3.508873	18.87305	29.15571	29.25565	16.1884	2.810449
h8	3.62974	18.97795	28.95788	28.64206	15.94644	2.866852
h9	3.818942	19.44268	28.83559	28.54627	16.18073	2.959547
h10	4.054309	20.19003	29.15571	28.93334	16.66244	3.07746
avg, **h_{52}**	3.62461	19.7469	31.2681	31.2723	17.3234	2.99595

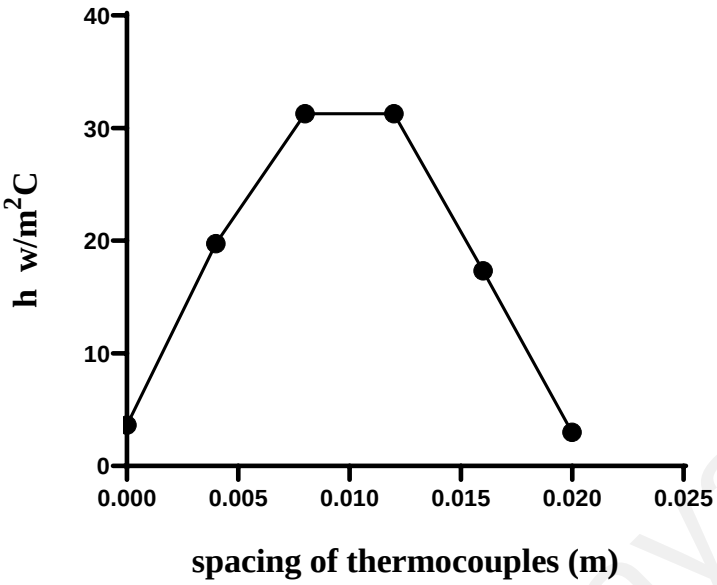

Figure 4.13: h_{52} versus spacing for Velocity 2.3m/s

The heat transfer coefficient values h_{52} of the design 2 for the velocity 2.3m/s are tabulated and the results are plotted in the graph. The Reynolds number for this flow was approximately above 33866 and is the maximum velocity. The heat transfer coefficient at the heater regions for this velocity were also same and moving towards the center the heat transfer coefficient increases gradually. The heat transfer at the center was found to be nearly same and this is supposed to be the velocity of the flow hitting the specimen was flat at this region. The heat transfer characteristics for the design 1 and design 2 were completely different that the shows the effect of air gap between the aluminum fins.

4.4 Average heat transfer coefficient

The average heat transfer coefficient for the Design 1 and Design 2 ranging from the minimum to maximum velocity was evaluated and analyzed for each localized points in the heat exchanger.

4.4.1 Design 1

The figure below is the average heat transfer coefficient **H_{11}** to **H_{51}** for the compact metal foams of design 1.

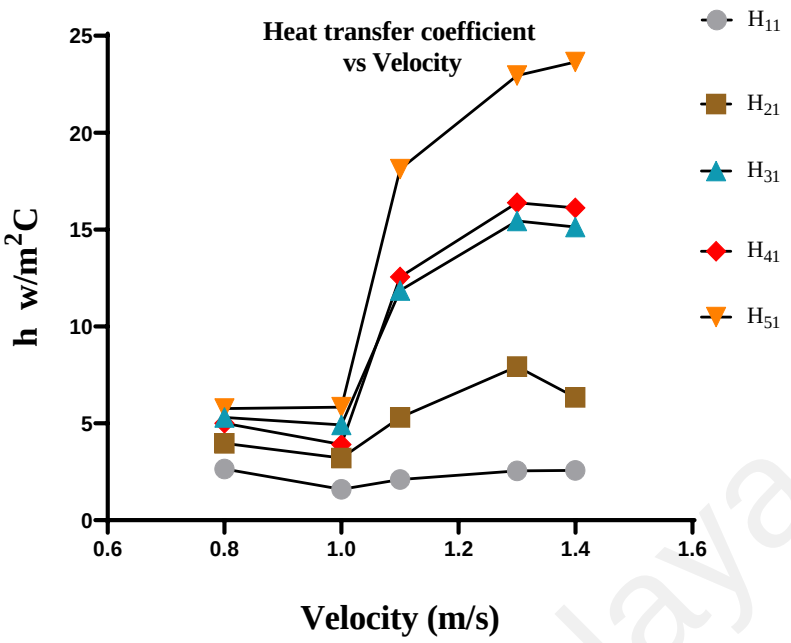

Figure 4.14: average H versus Velocity – Design 1

The average heat transfer coefficient for design 1 has been plotted for the localized points **h_{11}** to **h_{51}** for the different velocities. The experiments were conducted in steady state condition of giving the constant heat flux to the heater. The Figure 4.14 shows that the heat transfer coefficient increases from bottom to top as the velocity also increases. The localized point h_{11} is the first point in the heat exchanger where the thermocouples are located at periodic interval of 40mm until the top of the heat exchanger. It is observed that the heat transfer coefficient is smaller than the top and bottom of the heater regions for all the velocities. The heat transfer coefficient increases when the localized is moved along the heat exchanger towards the top. The design 1 of closely packed metal foams show this type of observation. Another observation that has the effect is the velocity profile which was higher at the top and the bottom was lower for which the heat transfer coefficient increases from the first point.

4.4.2 Design 2

The figure below is the average heat transfer coefficient **H_{12}** to **H_{52}** for the compact metal foams of design 2.

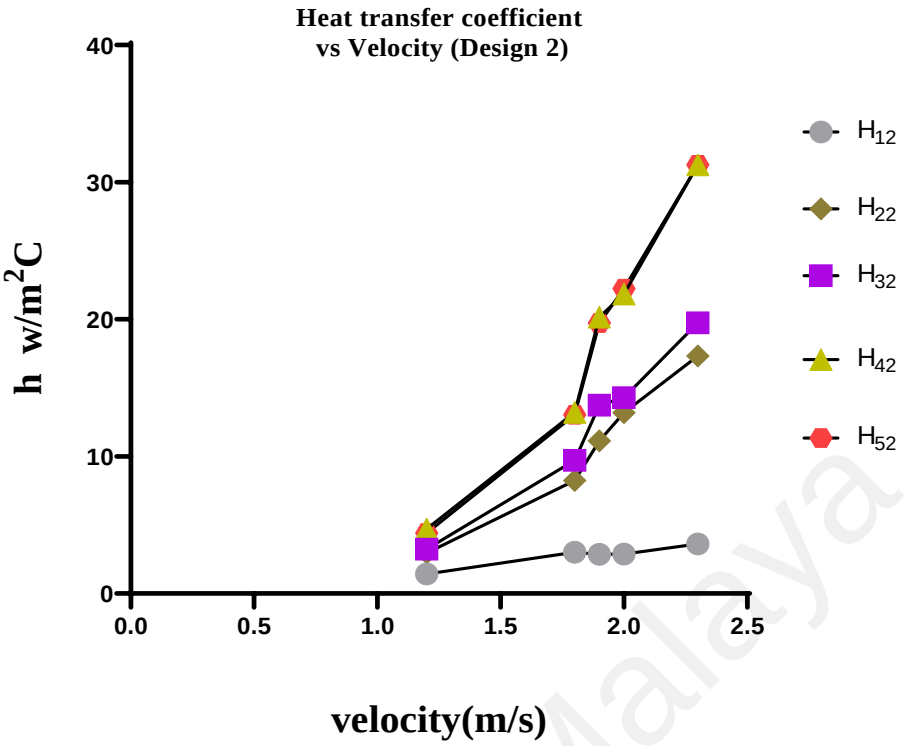

Figure 4.15: Average H versus Velocity - Design 2

The average heat transfer coefficient for design 2 has been plotted for the localized points $\mathbf{h_{12}}$ to $\mathbf{h_{52}}$ for the different velocities. The experiments were conducted in steady state condition of giving the constant heat flux to the heater. The Figure 4.15 shows that the heat transfer coefficient increases from bottom to top as the velocity also increases. The localized point h_{12} is the first point in the heat exchanger where the thermocouples are located at periodic interval of 40mm until the top of the heat exchanger. It is observed that the heat transfer coefficient increases from the bottom to top at all the localized points. The heat transfer at the top were seemed to same at both the points for this maximum velocity. It is completely different from the design 1 that has increase and decrease between the points of the same velocity. The effect of air gap of 5mm in between the aluminum fins were observed that the heat transfer coefficient towards the top show increase at the maximum velocity.

4.5 Bulk fluid temperature

The bulk fluid temperature and the temperature difference values area tabulated below for the design 1 and design 2.

Table 4.15: Temperature difference and Bulk fluid temperature – Design 1

Velocity (m/s)	Inlet temperature, T_{in} (˚C)	Outlet temperature, T_{out} (˚C)	ΔT (˚C)	Bulk fluid temperature, T_b
0.8	27.547	40.24	14.7	20.12
1	22.034	42.33	20.3	21.167
1.1	19.678	36.0778	16.4	18.039
1.3	20.181	36.28	16.1	18.14
1.4	19.983	35.78	15.8	17.89

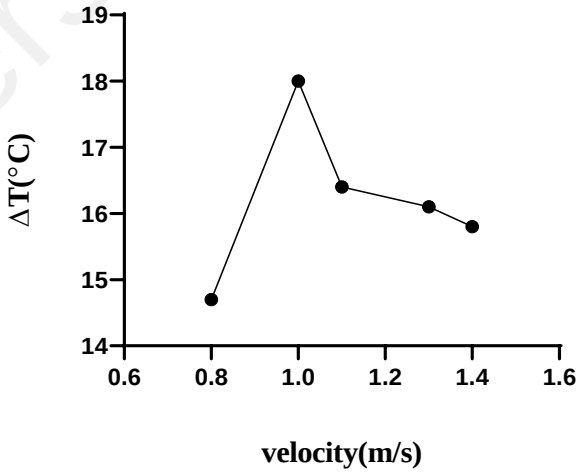

Figure 4.16: ΔT versus Velocity m/s – Design 1

The Inlet, Outlet temperatures for the design 1 at different velocity from minimum to maximum are tabulated. The temperature difference and the Bulk mean fluid temperature

were also evaluated. The Figure 4.16 shows the graph plotted for the temperature difference and the velocity at different points. It is observed that at the minimum velocity the inlet and outlet temperature difference is low. As the velocity increases the temperature difference decreases that is indirectly proportional. The temperature difference at the maximum velocity seems to be lower value when compared to other velocities. The Design 1 is closely packed metal foam heat exchanger therefore the fluid flow hitting the specimen will not escape easily and will hit at all the places. The heat transfer area for the design 1 is also high when compared to design 2. When reaching the maximum velocity temperature difference has only slight change. The bulk mean fluid temperature is observed to be higher at the lower velocity and lower at the higher velocity. The bulk temperature lies between 28˚-38˚C from the minimum velocity.

Table 4.16: Temperature difference and Bulk fluid temperature – Design 2

Velocity (m/s)	**Inlet temperature (˚C)**	**Outlet temperature (˚C)**	**ΔT (T_{out} - T_{in}) (˚C)**	**Bulk fluid temperature,**
1.2	28.5233	35.023	6.5	17.51
1.8	28.529	32.42	3.9	16.21
1.9	27.3723	30.87	3.5	15.43
2	28.161	31.361	3.2	15.68
2.3	28.1147	31.01	2.9	15.5

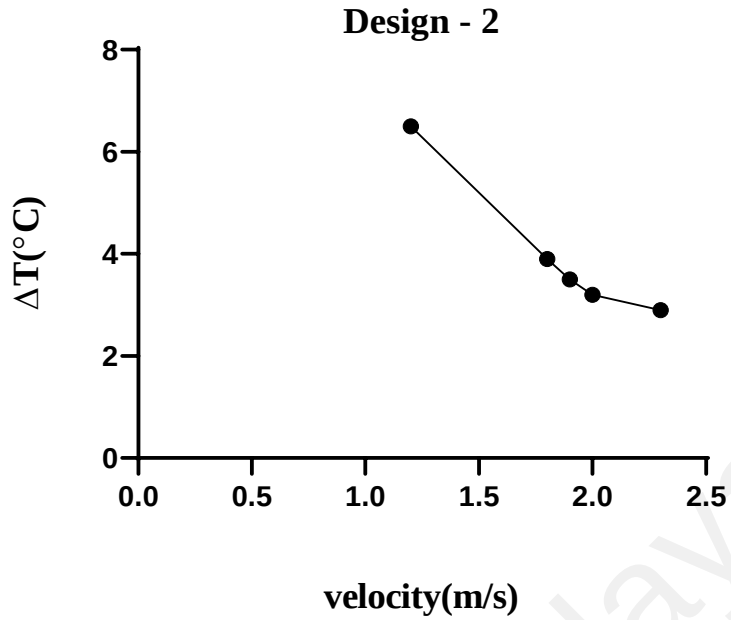

Figure 4.17: ΔT versus Velocity m/s – Design 2

The Inlet, Outlet temperatures for the design 2 at different velocity from minimum to maximum are tabulated. The temperature difference and the Bulk mean fluid temperature were also evaluated. The Figure 4.17 shows the graph plotted for the temperature difference and the velocity at different points. It is observed that the temperature difference of the inlet and outlet is very minimum when compared to design 1 lower velocity temperature difference. The temperature difference decreases gradually at each velocity and at the maximum velocity the temperature difference reaches minimum. The design 2 is metal foams packed with air gap of 5mm in between for the low temperature difference is observed. The heat transfer area for this design is less when compared to design 1 and also the fluid flow hitting the specimen can escape easily through the air gap that can slide. The bulk fluid temperature for this design lies between 29˚-33˚C where the range is very less. It is also observed that the temperature difference decreases with increase in velocity that can be high or low difference.

4.6 Nusselt number correlation

The Nusselt number is a non-dimensional number and is a function of heat transfer coefficient. the Nusselt number was calculated for both the design and is compared with literature paper.

Table 4.17: Evaluation of experimental Nusselt number

Velocity-Design 1 (m/s)	Velocity-Design 2 (m/s)	Reynolds number Design 1	Reynolds number Design 2	Experimental		Analytical Nusselt Number(Nu_A)
				Design 1 Nu_1	Design 2 Nu_2	
1.3	1.2	19142.12	17669.65	20.69	24.889	36.63
2.7	1.8	39756.7	26504.48	48.25	109.507	43.79
3.7	1.9	54481.4	27976.95	94.93	164.42	47.26
3.9	2	57426.4	29449.42	137.57	163.532	54.01
4	2.3	58898.8	33866.83	97.33	95.29	56.31

The Figure 4.18 below shows the Nusselt number correlation for present and previous study compared together with mathematical modelling.

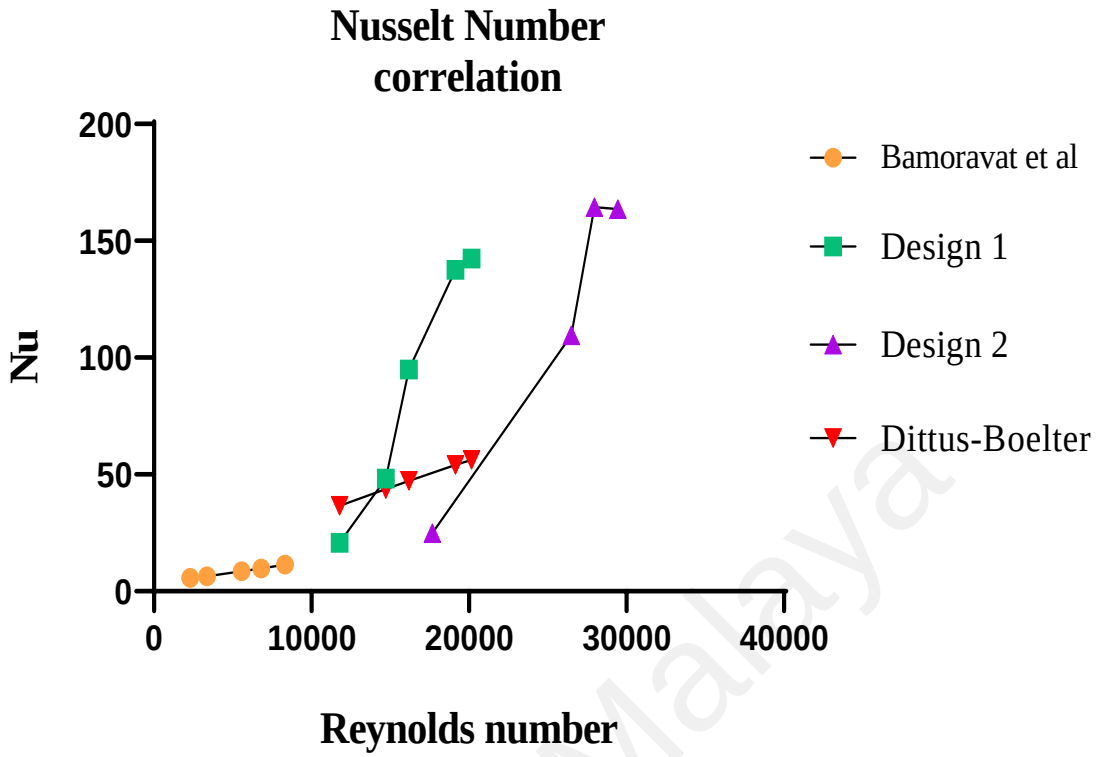

Figure 4.18: Comparison of Nusselt number between present and previous study

The Nusselt number was evaluated and tabulated for the experimental and analytical values for Design 1 and Design 2. (Bamorovat Abadi & Kim, 2017) in their have developed a heat transfer in small tubes which was based on low Reynolds number applications. The working fluid was the R245a refrigerant with the mass flux 200 to 1000kg/m^2. The metal foam porosity was reported as 0.9 with 30 PPI filled inside the hollow tube that was copper. The experiments were conducted in single phase where the heat flux do not have much effect on the Nusselt number. The Nusselt number correlations for different model has been conducted that doesn't coordinate with the experimental Nusselt number. The maximum Reynolds number was found to be approximately above 8324 that comes under laminar flow. This study has also developed the metal foam filled in the pipe for the low Reynolds number applications.

The Nusselt number evaluated in the present study is correlated with the previous literature work. The present study was evaluated for high range of Reynolds number for both Design 1 and 2. The Nusselt number for the design 1 was evaluated at the low Reynolds number where as the Nusselt number for the design 2 was evaluated at the higher range of Reynolds Number. The effect of the closely packed metal foams and the with the air gap show the effect in the Nusselt number correlation. The Nusselt number in the design 1 increases with the increase in Reynolds number and for the design 2 there was decrease at the higher range as the fluid passing has not effect on the heat transfer. The Nusselt number at each localized point evaluated shows the increase for both design. This is observed because the heater has placed at the top also and the Reynolds number has affected the heat transfer at this region. The velocity profile shown earlier was not flat that was also one of the factors that heat transfer decrease at this region. When overlapping both the design at some point the design 1 shows higher heat transfer than design 2 also the Reynolds number for the design 1 is lower and design 2 is higher. This is observed because the design 1 has low thermal resistance as the metal foams are closely packed the fluid passing has better heat transfer. Incase of design 2 the air gap provides high thermal resistance where the heat conduction was reduced. The fluid passing through it slides easily with the air gap with less heat transfer. Further adding to this the Nusselt number for the mathematical model equation called Dittus – Boelter was also evaluated and the results show the increase in difference between the mathematical modeling and the design correlation. The porosity of the pores, hollow ligament geometry, Reynolds number of the working fluid were all the possible factors that influence the high heat transfer.

CHAPTER 5: CONCLUSIONS

The present study has been conducted with achieving the objectives set for this research. The different configuration of developing the two different Designs of same PPI and porosity have been achieved. The heat transfer and the pressure drop characteristics was also studied. Firstly, the velocity profile of the test section with the specimen was evaluated that shows the fluid flow hitting the specimen. This is also one of the fact that the heat transfer is not same for all the localized points in the heat exchanger. The pressure drop for both the design were analyzed that shows difference in two designs. The pressure drop for design 1 was much higher than the design 2 that was because the first design had the metal foams closely packed with each other. The pressure drops in design 2 was lower when compared and this was because of the air gap in between the foams. The heat transfer coefficient for each localized point was studied for $\mathbf{H_{11}}$ to $\mathbf{H_{51}}$ and $\mathbf{H_{12}}$ to $\mathbf{H_{52}}$ for both the design. The heat transfer characteristics follow the similar pattern for points in design 1 and the design 2. This shows the Reynolds number effect the fluid flow inside the test section. The average heat transfer evaluated for both the designs increases with the increase in Reynolds number that means at low Reynolds number the heat transfer will be low. The fact is that the average heat transfer for the design increased compared to the design 1. The heat transfer area also was less in the design 2 and this is also the fact the average heat transfer was decreased. The temperature difference for the design 1 is also higher that means heat transferred to the fluid is high. In the case of design 2 the temperature difference was quite low that means the heat is absorbed by the fluid in the test section is low and the majority amount of fluid passed through the air gap. The bulk temperature also lies in the same region for both the design. The Nusselt number evaluation was conducted for both the design 1 and 2 and was compared with the literature paper. The literature evaluated the metal foam in low Reynolds number and the present study deals with the higher range of Reynolds number. the Nusselt number for the design

1 and 2 lies in the same region for evaluated values. The literature paper has lower range of Nusselt number because of the low Reynolds number effect. It is fact that increasing the Reynolds number increases the heat transfer. This shows that the design 1 has higher heat transfer are with high heat transfer in the low Reynolds number where as the design 2 has less heat transfer area and also the heat transferred to the fluid was less. The present study also lies in the same region of low Reynolds number because the Temperature Interface Material (TIM) has affected. The TIM was only placed at the heater region on top and bottom of the heat exchanger. The bonding between the metal foam fins were left usual that means with the help of clamping the force was given between the both. It is evident that the heat conduction between the copper and the aluminium fins were not high and placing the Temperature Interface Material within the copper and fins can increase the heat conduction greater whereby the heat transfer in the test section will also be higher.

5.1 FUTURE WORKS

- Due to the time constraint the present research was limited to only two different design of same porosity.
- The development of different design outcomes can be done to compare the efficiencies in between the different design. The porosity or PPI can be changed to see the effect of porosity in terms of heat transfer.
- The usage of the TIM within two material types can be increased for the design as the TIM posses higher heat transfer.
- The metal foams can be placed in an inclined angle of 45˚ against the fluid flow to see the effects. As the inclination of the metal foam has considerably higher effect this could be done.
- The evaluation of minimizing the area of metal foam and maximizing the heat transfer can be evaluated with many other different configuration arrangements.

REFERENCES

Bai, M., & Chung, J. N. (2011). Analytical and numerical prediction of heat transfer and pressure drop in open-cell metal foams. *International Journal of Thermal Sciences, 50*(6), 869-880. doi:https://doi.org/10.1016/j.ijthermalsci.2011.01.007

Bai, Q., Guo, Z., Cui, X., Yang, X., Yanhua, L., Jin, L., & Sun, Y. (2018). Experimental investigation on the solidification rate of water in open-cell metal foam with copper fins. *Energy Procedia, 152*, 210-214. doi:https://doi.org/10.1016/j.egypro.2018.09.082

Bamorovat Abadi, G., & Kim, K. C. (2017). Experimental heat transfer and pressure drop in a metal-foam-filled tube heat exchanger. *Experimental Thermal and Fluid Science, 82*, 42-49. doi:https://doi.org/10.1016/j.expthermflusci.2016.10.031

Beer, M., Rybár, R., & Kaľavský, M. (2019). Experimental heat transfer analysis of open cell hollow ligament metal foam at low Reynolds number. *Measurement, 133*, 214-221. doi:https://doi.org/10.1016/j.measurement.2018.10.025

Boomsma, K., Poulikakos, D., & Zwick, F. (2003). Metal foams as compact high performance heat exchangers. *Mechanics of Materials, 35*(12), 1161-1176. doi:https://doi.org/10.1016/j.mechmat.2003.02.001

Buonomo, B., Pasqua, A. d., Ercole, D., & Manca, O. (2018). Numerical investigation on a Heat Exchanger in Aluminum Foam. *Energy Procedia, 148*, 782-789. doi:https://doi.org/10.1016/j.egypro.2018.08.132

Diani, A., Bodla, K. K., Rossetto, L., & Garimella, S. V. (2015). Numerical investigation of pressure drop and heat transfer through reconstructed metal foams and comparison against experiments. *International Journal of Heat and Mass Transfer, 88*, 508-515. doi:https://doi.org/10.1016/j.ijheatmasstransfer.2015.04.038

Hamadouche, A., Nebbali, R., Benahmed, H., Kouidri, A., & Bousri, A. (2016). Experimental investigation of convective heat transfer in an open-cell aluminum foams. *Experimental Thermal and Fluid Science, 71*, 86-94. doi:https://doi.org/10.1016/j.expthermflusci.2015.10.009

Hu, H., Lai, Z., & Ding, G. (2018). Heat transfer and pressure drop characteristics of wet air flow in metal foam with hydrophobic coating under dehumidifying conditions. *Applied Thermal Engineering, 132*, 651-664. doi:https://doi.org/10.1016/j.applthermaleng.2018.01.010

Huisseune, H., De Schampheleire, S., Ameel, B., & De Paepe, M. (2015). Comparison of metal foam heat exchangers to a finned heat exchanger for low Reynolds number applications. *International Journal of Heat and Mass Transfer, 89*, 1-9. doi:https://doi.org/10.1016/j.ijheatmasstransfer.2015.05.013

Iasiello, M., Bianco, N., Chiu, W. K. S., & Naso, V. (2019). Thermal conduction in open-cell metal foams: Anisotropy and Representative Volume Element. *International*

Journal of Thermal Sciences, 137, 399-409. doi:https://doi.org/10.1016/j.ijthermalsci.2018.12.002

Javadi, H., Mousavi Ajarostaghi, S. S., Pourfallah, M., & Zaboli, M. (2019). Performance analysis of helical ground heat exchangers with different configurations. *Applied Thermal Engineering, 154,* 24-36. doi:https://doi.org/10.1016/j.applthermaleng.2019.03.021

Kopanidis, A., Theodorakakos, A., Gavaises, E., & Bouris, D. (2010). 3D numerical simulation of flow and conjugate heat transfer through a pore scale model of high porosity open cell metal foam. *International Journal of Heat and Mass Transfer, 53*(11), 2539-2550. doi:https://doi.org/10.1016/j.ijheatmasstransfer.2009.12.067

Labat, M., Virgone, J., David, D., & Kuznik, F. (2014). Experimental assessment of a PCM to air heat exchanger storage system for building ventilation application. *Applied Thermal Engineering, 66*(1), 375-382. doi:https://doi.org/10.1016/j.applthermaleng.2014.02.025

Lai, Z., Hu, H., & Ding, G. (2018). Effect of porosity on heat transfer and pressure drop characteristics of wet air in hydrophobic metal foam under dehumidifying conditions. *Experimental Thermal and Fluid Science, 96,* 90-100. doi:https://doi.org/10.1016/j.expthermflusci.2018.02.025

Ma, J., Lv, P., Luo, X., Liu, Y., Li, H., & Wen, J. (2016). Experimental investigation of flow and heat transfer characteristics in double-laminated sintered woven wire mesh. *Applied Thermal Engineering, 95,* 53-61. doi:https://doi.org/10.1016/j.applthermaleng.2015.11.015

Mancin, S., Zilio, C., Diani, A., & Rossetto, L. (2012). Experimental air heat transfer and pressure drop through copper foams. *Experimental Thermal and Fluid Science, 36,* 224-232. doi:https://doi.org/10.1016/j.expthermflusci.2011.09.016

Nawaz, K., Bock, J., & Jacobi, A. M. (2017). Thermal-hydraulic performance of metal foam heat exchangers under dry operating conditions. *Applied Thermal Engineering, 119,* 222-232. doi:https://doi.org/10.1016/j.applthermaleng.2017.03.056

P. Elayiaraja, S. H., L. Wilson, A. Bensely & D. M. Lal (2010). (July 2010). Experimental Investigation on Pressure Drop and Heat Transfer Characteristics of Copper Metal Foam Heat Sink. *Experimental Heat Transfer: A Journal of Thermal Energy Generation, Transport, Storage, and conversion.*

Rao, Z., Wen, Y., & Liu, C. (2018). Enhancement of heat transfer of microcapsulated particles using copper particles and copper foam. *Particuology, 41,* 85-93. doi:https://doi.org/10.1016/j.partic.2017.12.010

Samana, T., Kiatsiriroat, T., & Nuntaphan, A. (2014). Enhancement of fin efficiency of a solid wire fin by oscillating heat pipe under forced convection. *Case Studies in Thermal Engineering, 2,* 36-41. doi:https://doi.org/10.1016/j.csite.2013.10.003

Shi, J., Zheng, G., Chen, Z., & Dang, C. (2019). Experimental study of flow condensation heat transfer in tubes partially filled with hydrophobic annular metal foam.

International Journal of Heat and Mass Transfer, 136, 1265-1272. doi:https://doi.org/10.1016/j.ijheatmasstransfer.2019.03.039

Tiwari, R., Andhare, R. S., Shooshtari, A., & Ohadi, M. (2019). Development of an additive manufacturing-enabled compact manifold microchannel heat exchanger. *Applied Thermal Engineering, 147*, 781-788. doi:https://doi.org/10.1016/j.applthermaleng.2018.10.122

Wang, H., & Guo, L. (2016). Experimental investigation on pressure drop and heat transfer in metal foam filled tubes under convective boundary condition. *Chemical Engineering Science, 155*, 438-448. doi:https://doi.org/10.1016/j.ces.2016.08.031

Wang, J., Kong, H., Xu, Y., & Wu, J. (2019). Experimental investigation of heat transfer and flow characteristics in finned copper foam heat sinks subjected to jet impingement cooling. *Applied Energy, 241*, 433-443. doi:https://doi.org/10.1016/j.apenergy.2019.03.040

Yunus A.cengel, A. J. G. (2016). *Heat and Mass transfer*. New delhi: McGraw Hill Educationn pvt.ltd.